

Non-monotonicity in Conformal Risk Control

Tareq Aldirawi, Yun Li, and Wenge Guo*

Department of Mathematical Sciences
New Jersey Institute of Technology, Newark, NJ, USA

Abstract

Conformal risk control (CRC) provides distribution-free guarantees for controlling the expected loss at a user-specified level. Existing theory typically assumes that the loss decreases monotonically with a tuning parameter that governs the size of the prediction set. This assumption is often violated in practice, where losses may behave non-monotonically due to competing objectives such as coverage and efficiency.

We study CRC under non-monotone loss functions when the tuning parameter is selected from a finite grid, a common scenario in thresholding or discretized decision rules. Revisiting a known counterexample, we show that the validity of CRC without monotonicity depends on the relationship between the calibration sample size and the grid resolution. In particular, risk control can still be achieved when the calibration sample is sufficiently large relative to the grid.

We provide a finite-sample guarantee for bounded losses over a grid of size m , showing that the excess risk above the target level α is of order $\sqrt{\log(m)/n}$, where n is the calibration sample size. A matching lower bound shows that this rate is minimax optimal. We also derive refined guarantees under additional structural conditions, including Lipschitz continuity and monotonicity, and extend the analysis to settings with distribution shift via importance weighting.

Numerical experiments on synthetic multilabel classification and real object detection data illustrate the practical impact of non-monotonicity. Methods that account for finite-sample deviations achieve more stable risk control than approaches based on monotonicity transformations, while maintaining competitive prediction-set sizes.

Keywords: conformal prediction; risk control; nonmonotone loss; finite-sample properties; minimax theory; distribution-free methods.

1 Introduction

Uncertainty quantification is essential in high-stakes prediction tasks, including medical diagnosis, autonomous systems, and scientific decision-making. While point predictions may achieve high

*Author e-mail addresses: ta429@njit.edu; yl238@njit.edu; wenge.guo@njit.edu

accuracy, practitioners often require calibrated measures of uncertainty. Conformal prediction addresses this need by constructing prediction sets with finite-sample coverage guarantees under the mild assumption of exchangeability Vovk et al. [1999, 2005], Papadopoulos et al. [2002]. However, coverage is not always the most relevant performance criterion. In many applications, practitioners instead seek to control other risk functionals, such as precision in information retrieval, false negative rates in medical screening, or fairness-related metrics in algorithmic decision-making.

Conformal risk control (CRC) Angelopoulos et al. [2024b] extends the conformal prediction framework to provide distribution-free guarantees for controlling user-specified risks in expectation. We briefly review the CRC setup. Let

$$D_{1:n+1} = ((X_1, Y_1), \dots, (X_{n+1}, Y_{n+1})) \in (\mathcal{X} \times \mathcal{Y})^{n+1}$$

be exchangeable random variables with joint distribution \mathbb{P} . Given a calibration dataset $D_{1:n}$ and a test covariate X_{n+1} , the goal is to construct a prediction set for the unknown response Y_{n+1} .

Let $\mathcal{C} : \mathcal{X} \times \Lambda \rightarrow 2^{\mathcal{Y}}$ denote a prediction-set function indexed by $\lambda \in \Lambda \subseteq \mathbb{R}$. The parameter λ controls the size of the prediction set, and we assume the monotonicity property

$$\lambda_1 \leq \lambda_2 \Rightarrow \mathcal{C}(x; \lambda_1) \subseteq \mathcal{C}(x; \lambda_2) \quad \text{for all } x \in \mathcal{X}.$$

Let $\ell : \mathcal{X} \times \mathcal{Y} \times \Lambda \rightarrow [0, B]$ be a bounded loss function with $B < \infty$. The objective is to select $\hat{\lambda} \in \Lambda$ based on $D_{1:n}$ such that

$$\mathbb{E} \left[\ell(X_{n+1}, Y_{n+1}; \hat{\lambda}) \right] \leq \alpha, \tag{1}$$

for a user-specified risk level $\alpha \in (0, 1)$.

Under the additional assumption that $\ell(x, y; \lambda)$ is non-increasing in λ for all (x, y) , CRC selects the parameter

$$\hat{\lambda} = \inf \left\{ \lambda \in \Lambda : \frac{1}{n+1} \left(\sum_{i=1}^n \ell(X_i, Y_i; \lambda) + B \right) \leq \alpha \right\}. \tag{2}$$

This construction accounts for the worst-case contribution of the test observation and yields the guarantee in (1) under exchangeability and monotonicity.

While this framework is general, the monotonicity assumption on the loss function may fail in practice. For example, in object detection, controlling error rates requires balancing false positives and true detections, leading to losses that are typically non-monotonic in the score threshold λ . Similarly, in medical screening with multiple diagnostic criteria, expanding the decision rule may reduce some errors while increasing others, so the overall loss need not decrease with λ . When the loss is non-monotonic, the standard CRC guarantee may fail, as illustrated by a counterexample in Angelopoulos et al. [2024b].

In this paper, we revisit this setting and focus on the practically important case where the parameter space is a finite discrete grid

$$\Lambda = \{\lambda_1, \dots, \lambda_m\},$$

as arises when tuning a score threshold or decision rule over a set of candidate values. We show that, even without monotonicity, CRC can still achieve approximate risk control when the calibration sample size is sufficiently large relative to the grid size. Our main finite-sample guarantee shows that

$$\mathbb{E}\left[\ell(X_{n+1}, Y_{n+1}; \hat{\lambda})\right] \leq \alpha + C\sqrt{\frac{\log m}{n}},$$

for a universal constant $C > 0$. We further prove a matching lower bound showing that this rate is minimax optimal.

We also investigate structural assumptions on the loss function that lead to improved guarantees: Lipschitz losses yield faster convergence rates under a margin condition, while monotone losses recover the classical CRC guarantee. Finally, we extend the analysis to settings with distribution shift using importance weighting.

These results demonstrate that monotonicity is not essential for effective conformal risk control in discretized settings, provided that the calibration sample size is sufficiently large relative to the parameter grid.

Contributions. Our main contributions are as follows.

1. We analyze conformal risk control when the loss function is non-monotonic in the prediction set parameter. Revisiting a counterexample from the CRC literature, we show that the behavior of CRC depends critically on the interplay between the calibration sample size and the resolution of the parameter grid.
2. For bounded losses over a finite grid $\Lambda = \{\lambda_1, \dots, \lambda_m\}$, we establish a finite-sample guarantee showing that the excess risk above the target level α is of order $\sqrt{\log(m)/n}$.
3. We prove a matching lower bound demonstrating that the $\sqrt{\log(m)/n}$ rate is minimax optimal in general.
4. We obtain refined guarantees under structural assumptions on the loss function, including Lipschitz losses and monotone losses.
5. We extend the framework to settings with distribution shift using importance weighting and provide empirical evaluations on synthetic and real-world benchmarks.

Organization of the paper. Section 2 reviews related work. Section 3.1 revisits the counterexample illustrating the failure of CRC under non-monotonic losses. Sections 3.2–3.3 present our main finite-sample guarantees and the corresponding minimax lower bound. Section 4 studies refined guarantees under structural assumptions on the loss function, while Section 5 compares our approach with existing methods for handling non-monotonic losses. Section 7 extends the framework to settings with distribution shift, and Section 6 presents empirical results.

2 Related Work

Conformal prediction, introduced by Vovk, Gammerman, and collaborators Vovk et al. [1999, 2005], provides model-agnostic uncertainty quantification with finite-sample coverage guarantees under exchangeability. Split conformal prediction Papadopoulos et al. [2002] offers a computationally efficient variant based on a held-out calibration set, with statistical properties studied in Lei et al. [2018]. Comprehensive introductions can be found in Angelopoulos and Bates [2021], Shafer and Vovk [2008], and recent developments are surveyed in Angelopoulos et al. [2024a]. Extensions beyond exchangeability Tibshirani et al. [2019], Podkopaev and Ramdas [2021], Barber et al. [2023] and results on conditional coverage Vovk [2012], Foygel Barber et al. [2021], Gibbs et al. [2025] further broaden the scope of conformal inference.

Building on this literature, recent work has developed conformal methods for controlling more general risk functionals. Risk-controlling prediction sets (RCPS) Bates et al. [2021] provide high-probability bounds on user-specified risks under monotone loss functions. The learn-then-test (LTT) framework Angelopoulos et al. [2025] introduces a modular two-stage procedure based on multiple testing, which can accommodate non-monotone loss functions. Conformal risk control (CRC) Angelopoulos et al. [2024b] offers an alternative conformal framework that controls risk in expectation for monotone losses. Compared with RCPS, which provides high-probability guarantees, CRC controls risk in expectation and can therefore yield less conservative procedures. Standard split conformal prediction can be viewed as a special case of CRC. Several extensions of CRC have subsequently been proposed, including cross-validation and leave-one-out variants Cohen et al. [2024], full conformal risk control Angelopoulos [2024], and weighted methods for non-exchangeable settings Farinhas et al. [2023]. Applications to modern machine learning tasks include Schuster et al. [2021], Fisch et al. [2022], Angelopoulos et al. [2022], Feldman et al. [2022], Teneggi et al. [2023]. Recently, Angelopoulos Angelopoulos [2026] proposed stability-based approaches for handling non-monotonicity in CRC by imposing structural assumptions on the learning algorithm rather than on the loss function.

Our work takes a complementary perspective. Instead of relying on algorithmic stability, we analyze the statistical error induced by selecting the prediction-set parameter over a finite grid. For bounded loss functions, including non-monotone ones, we derive finite-sample guarantees that explicitly bound the excess risk above the target level. In contrast to LTT, our guarantees are formulated in expectation, and unlike standard CRC, our analysis does not require monotonicity of the loss. Our results show that the excess risk incurred by searching over a finite parameter grid scales logarithmically with the grid size. These results provide a complementary perspective on non-monotonicity, showing that it can be addressed through statistical analysis of the selection procedure rather than through structural assumptions.

3 Main Results

We study conformal risk control under non-monotonic losses. Section 3.1 revisits the counterexample from Angelopoulos et al. [2024b] and sharpens its implications. Section 3.2 develops finite-sample expectation bounds for discrete parameter sets, while Sections 3.3–5.1 provide complementary lower bounds and efficiency comparisons.

3.1 Counterexample Analysis

Write $L_i(\lambda) := \ell(X_i, Y_i; \lambda)$. We restate the counterexample from Angelopoulos et al. [2024b] and quantify its behavior as the grid size m grows. Let $B = 1$, $\Lambda = \{0, 1/m, \dots, 1\}$, $\alpha \in (1/(n+1), 1)$, and $p \in (\alpha, 1)$. For $j < m$, define $L_i(j/m) \stackrel{\text{i.i.d.}}{\sim} \text{Bern}(p)$ and $L_i(1) = 0$, independent across i and j . Thus the loss is non-monotonic since $\mathbb{E}[L_i(j/m)] = p$ for $j < m$ but $\mathbb{E}[L_i(1)] = 0$.

Since $B = 1$, the CRC threshold (2) reduces to

$$\hat{\lambda} = \inf \left\{ \lambda \in \Lambda : \frac{1}{n+1} \sum_{i=1}^n L_i(\lambda) + \frac{1}{n+1} \leq \alpha \right\},$$

with $\inf \emptyset = 1$. Since $\hat{\lambda}$ depends only on $D_{1:n}$, it is independent of $L_{n+1}(\cdot)$. Because $L_{n+1}(1) = 0$ and $L_{n+1}(j/m) \sim \text{Bern}(p)$ for $j < m$,

$$\mathbb{E}[L_{n+1}(\hat{\lambda})] = p \mathbb{P}(\hat{\lambda} \neq 1).$$

Let

$$q = \mathbb{P} \left(\frac{1}{n} \sum_{i=1}^n Z_i \leq \alpha - \frac{1}{n+1} \right), \quad Z_i \sim \text{Bern}(p).$$

Independence across grid points implies

$$\mathbb{P}(\hat{\lambda} = 1) = (1 - q)^m,$$

so

$$\mathbb{E}[L_{n+1}(\hat{\lambda})] = p(1 - (1 - q)^m). \tag{3}$$

Using the bounds $1 - mq \leq (1 - q)^m \leq e^{-mq}$, we obtain

$$p(1 - e^{-mq}) \leq \mathbb{E}[L_{n+1}(\hat{\lambda})] \leq pmq.$$

Let

$$S_n = \sum_{i=1}^n Z_i \sim \text{Bin}(n, p), \quad t = \alpha - \frac{1}{n+1},$$

so that

$$q = \mathbb{P} \left(\frac{S_n}{n} \leq t \right).$$

For the upper bound, Hoeffding's inequality yields

$$q \leq \exp(-2n(p-t)^2), \quad \text{since } 0 < t < p.$$

For a simple lower bound, note that

$$q \geq \mathbb{P}(S_n = 0) = (1-p)^n.$$

Substituting these bounds gives

$$p(1 - e^{-m(1-p)^n}) \leq \mathbb{E}[L_{n+1}(\hat{\lambda})] \leq pm \exp(-2n(p-t)^2).$$

The behavior exhibits a sharp scaling transition governed by the relation between n and $\log m$.

Risk is controlled if

$$pm e^{-2n(p-t)^2} \leq \alpha,$$

which holds when n grows at least on the order of $\log m$, e.g.

$$n \gtrsim \frac{\log m}{2(p-\alpha)^2}.$$

Risk is not controlled if

$$p(1 - e^{-m(1-p)^n}) > \alpha,$$

which occurs when

$$m(1-p)^n \gtrsim 1, \quad \text{equivalently } n \lesssim \frac{\log m}{-\log(1-p)}.$$

In the absence of monotonicity, risk control is no longer guaranteed; instead, it depends on the relative growth of the sample size n and the grid resolution m . In particular, increasing model resolution (larger m) can compromise risk control unless supported by sufficient data (larger n). As a result, risk control becomes a scaling-dependent property rather than an intrinsic guarantee. This highlights a fundamental limitation of existing conformal risk control methods and motivates the development of new algorithms capable of handling non-monotonic loss functions.

3.2 Main Result for Non-Monotonic Losses

We derive an upper bound on the expected non-monotonic losses over a finite parameter set $\Lambda = \{\lambda_1, \dots, \lambda_m\}$. By appropriately adjusting the pre-specified risk level, this leads to finite-sample expectation control for non-monotonic losses.

Throughout this section, we assume that for each $\lambda \in \Lambda$, the sequence $\{L_i(\lambda)\}_{i=1}^{n+1}$ is i.i.d. The analysis relies on Hoeffding's inequality. Let

$$R(\lambda) = \mathbb{E}[L_i(\lambda)], \quad \hat{R}_n(\lambda) = \frac{1}{n} \sum_{i=1}^n L_i(\lambda).$$

Theorem 1. *Suppose that for each $\lambda \in \Lambda$, $\{L_i(\lambda)\}_{i=1}^{n+1}$ are i.i.d. and satisfy*

$$0 \leq L_i(\lambda) \leq B \quad \text{almost surely.}$$

Assume there exists $\lambda^ \in \Lambda$ such that*

$$R(\lambda^*) \leq \alpha.$$

Define

$$\hat{\lambda} = \inf \left\{ \lambda \in \Lambda : \frac{n}{n+1} \hat{R}_n(\lambda) + \frac{B}{n+1} \leq \alpha \right\},$$

with the convention that $\inf \emptyset = \lambda_m$. Then

$$\mathbb{E}[L_{n+1}(\hat{\lambda})] \leq \alpha + D(m, n),$$

where

$$D(m, n) = B \sqrt{\frac{\log(2m)}{2n}} + \frac{B}{2\sqrt{2n \log(2m)}}.$$

In particular, applying the selection rule with the calibrated level $\alpha' = \alpha - D(m, n)$ yields

$$\hat{\lambda}^{\text{adj}} = \inf \left\{ \lambda \in \Lambda : \frac{n}{n+1} \hat{R}_n(\lambda) + \frac{B}{n+1} \leq \alpha' \right\},$$

which guarantees

$$\mathbb{E}[L_{n+1}(\hat{\lambda}^{\text{adj}})] \leq \alpha.$$

The proof (Appendix B) is based on a uniform concentration argument over Λ using Hoeffding's inequality, combined with a union bound to account for selection among the m candidate parameters.

Remark 1 (Feasibility). *The assumption $R(\lambda^*) \leq \alpha$ holds by construction. The grid Λ includes a maximally conservative choice λ_{\max} that outputs the full response set, yielding $L_i(\lambda_{\max}) = 0$ almost surely and hence $R(\lambda_{\max}) = 0 \leq \alpha$.*

Implications and Interpretation. The theorem provides a finite-sample expectation guarantee for non-monotonic losses, with an explicit excess term $D(m, n)$ capturing the statistical cost of model selection over a finite parameter set.

A fundamental trade-off emerges: increasing m improves resolution by reducing discretization error, but simultaneously enlarges the selection space and thus increases estimation uncertainty. Since this cost grows only logarithmically in m , moderately rich parameter grids remain effective when the sample size n is sufficiently large.

The guarantee relies only on mild assumptions: bounded losses, independence, and the existence of at least one candidate λ^* achieving the target risk level α . Under these conditions, the selected parameter $\hat{\lambda}$ attains near-target performance even in the absence of monotonicity.

Table 1: Excess term $D(m, n)$ for $m = 100$ and $m = 200$ ($B = 1$).

n	$m = 100$			$m = 200$		
	D	$D/0.1$	$D/0.2$	D	$D/0.1$	$D/0.2$
1,000	0.0563	0.5630	0.2815	0.0606	0.6060	0.3030
5,000	0.0252	0.2520	0.1260	0.0271	0.2710	0.1355
10,000	0.0178	0.1780	0.0890	0.0192	0.1920	0.0960
50,000	0.0080	0.0800	0.0400	0.0086	0.0860	0.0430
100,000	0.0056	0.0560	0.0280	0.0061	0.0610	0.0305

The bound $D(m, n)$ in Theorem 1 is derived using Hoeffding’s inequality, which depends on the range of the loss rather than its variance. When the loss distribution has low variance (i.e., is concentrated around its mean), this can be conservative. In Appendix C we develop variance-sensitive concentration inequalities that exploit the empirical variance of the losses, yielding tighter corrections when the loss distribution is concentrated.

Thus, risk control in the non-monotonic setting becomes resolution-dependent: finer parameter grids require larger sample sizes to maintain comparable statistical reliability. Table 1 illustrates the theoretical behavior of $D(m, n)$. The excess term decays at the expected $1/\sqrt{n}$ rate and depends only logarithmically on the grid size. Doubling the grid from $m = 100$ to $m = 200$ changes the bound only slightly, consistent with its logarithmic dependence on m .

More importantly, the inflation rate D/α becomes small once the calibration sample reaches a few thousand observations. For instance, when $\alpha = 0.2$ and $m = 100$, $n = 10,000$ yields $D \approx 0.019$, corresponding to $D/\alpha \approx 0.096$. At $n = 50,000$, the inflation rate drops to about $D/\alpha \approx 0.043$. Thus, the theoretical correction translates into only modest practical inflation at realistic sample sizes.

Discretization error. Let $\lambda_{\text{ora}} = \inf\{\lambda : R(\lambda) \leq \alpha\}$ denote the oracle threshold in the underlying continuous parameter space. If $\lambda_{\text{ora}} \notin \Lambda$, the grid-restricted oracle

$$\lambda_m^* = \inf\{\lambda \in \Lambda : R(\lambda) \leq \alpha\}$$

satisfies $\lambda_m^* \geq \lambda_{\text{ora}}$. Consequently, the selected parameter is necessarily more conservative than the true oracle, potentially resulting in larger prediction sets or higher loss.

This gap represents an intrinsic approximation error induced by the finite grid. As m increases, the grid becomes denser and λ_m^* moves closer to λ_{ora} , thereby reducing discretization bias. At the same time, expanding Λ increases the complexity of the selection problem, which in turn amplifies stochastic variability. This effect is captured by the excess term $D(m, n)$.

A fundamental discretization–selection trade-off therefore emerges: finer grids improve approximation to the continuous oracle but make reliable estimation more challenging, requiring larger sample sizes to control the additional variability. Thus, the choice of Λ must balance model resolution against statistical stability.

3.3 Lower Bound

We now show that the dependence $D(m, n) \approx \sqrt{\log m/n}$ in Theorem 1 is not specific to the CRC procedure, but reflects a fundamental difficulty inherent in selecting among m candidate levels using n samples. This difficulty already arises in the simplest setting of binary losses taking values in $\{0, 1\}$. The following lower bound, established for this case, holds uniformly over all measurable selection rules.

Proposition 1 (Lower bound). *Let n denote the number of calibration observations and $m \geq 4$ the size of the candidate grid used for selecting λ . Then there exists a distribution over binary loss vectors*

$$(L_i(\lambda_1), \dots, L_i(\lambda_m)) \in \{0, 1\}^m$$

such that the vectors are i.i.d. for $i = 1, \dots, n + 1$, and for any measurable selection rule $\hat{\lambda} = \hat{\lambda}(D_{1:n})$,

$$\mathbb{E}[L_{n+1}(\hat{\lambda})] \geq \alpha + c \sqrt{\frac{\log m}{n}},$$

where $c > 0$ is a universal constant independent of n and m .

Proposition 1 shows that the excess risk term in Theorem 1 is not an artifact of the CRC procedure, but reflects an intrinsic statistical difficulty of selecting among m candidate levels using n samples. Even with an oracle-designed data-driven method, the excess risk cannot be uniformly smaller than order $\sqrt{\log m/n}$ over bounded non-monotonic losses. Thus, the inflation incurred by CRC is not avoidable in general: it matches the fundamental statistical cost of selecting a level from finite data. Together with Theorem 1, this shows that CRC achieves the optimal worst-case rate up to constants.

4 Improved Risk Bounds under Structured Loss Functions

The excess term in Theorem 1 scales as $\mathcal{O}(\sqrt{\log m/n})$, reflecting uniform concentration over the finite class $\{L(\cdot, \lambda) : \lambda \in \Lambda\}$. This bound holds without structural assumptions on the loss function.

Stronger guarantees can be obtained when additional structure is imposed. In particular, smoothness assumptions lead to refined bounds that depend on the stability of the selected threshold, while monotonicity restores exact conformal risk control.

4.1 Refined Bounds under Lipschitz Loss

Assume that the loss function is K -Lipschitz in λ , that is, for all $\lambda_1, \lambda_2 \in \Lambda$,

$$|L_i(\lambda_1) - L_i(\lambda_2)| \leq K|\lambda_1 - \lambda_2|.$$

Recall that

$$\hat{\lambda} = \inf \left\{ \lambda \in \Lambda : \frac{n}{n+1} \hat{R}_n(\lambda) + \frac{B}{n+1} \leq \alpha \right\}, \quad \hat{\lambda}' = \inf \{ \lambda \in \Lambda : \hat{R}_{n+1}(\lambda) \leq \alpha \},$$

with the convention $\inf \emptyset = \lambda_m$.

Using the decomposition

$$\mathbb{E}[L_{n+1}(\hat{\lambda})] = \mathbb{E}[L_{n+1}(\hat{\lambda}')] + \Delta_n, \quad \Delta_n = \mathbb{E}\left[L_{n+1}(\hat{\lambda}) - L_{n+1}(\hat{\lambda}')\right],$$

the Lipschitz condition implies

$$|\Delta_n| \leq K \mathbb{E}\left[|\hat{\lambda} - \hat{\lambda}'|\right] \leq K \text{diam}(\Lambda) \mathbb{P}(\hat{\lambda} \neq \hat{\lambda}'),$$

where $\text{diam}(\Lambda) = \lambda_m - \lambda_1$.

Thus the excess risk is controlled by the probability that the two thresholds $\hat{\lambda}$ and $\hat{\lambda}'$ disagree. To bound this probability, suppose there exists $\lambda^* \in \Lambda$ and $\epsilon > 0$ such that

$$R(\lambda^*) \leq \alpha - \epsilon.$$

If $\epsilon \geq (B - \alpha)/n$, then

$$\mathbb{P}(\hat{\lambda} \neq \hat{\lambda}') \leq \exp\left(-\frac{2n\epsilon^2}{B^2}\right).$$

Combining these bounds yields the following result.

Proposition 2 (Lipschitz Refinement). *Suppose the assumptions of Theorem 1 hold. Assume additionally that the loss functions $L_i(\lambda)$ are K -Lipschitz in λ , i.e.,*

$$|L_i(\lambda_1) - L_i(\lambda_2)| \leq K|\lambda_1 - \lambda_2|, \quad \forall \lambda_1, \lambda_2 \in \Lambda.$$

Let $\text{diam}(\Lambda) = \lambda_m - \lambda_1$. Suppose there exists $\lambda^ \in \Lambda$ and $\epsilon > 0$ such that $R(\lambda^*) \leq \alpha - \epsilon$. Then*

$$\mathbb{E}[L_{n+1}(\hat{\lambda})] \leq \alpha + K \text{diam}(\Lambda) \mathbb{P}(\hat{\lambda} \neq \hat{\lambda}').$$

Moreover, if $\epsilon \geq (B - \alpha)/n$, then

$$\mathbb{P}(\hat{\lambda} \neq \hat{\lambda}') \leq \exp\left(-\frac{2n\epsilon^2}{B^2}\right),$$

and therefore

$$\mathbb{E}[L_{n+1}(\hat{\lambda})] \leq \alpha + K(\lambda_m - \lambda_1) \exp\left(-\frac{2n\epsilon^2}{B^2}\right).$$

Proposition 2 shows that under Lipschitz losses the excess risk is governed by the stability of the threshold selection procedure. When the oracle parameter λ^* achieves risk strictly below α , the probability that $\hat{\lambda}$ and $\hat{\lambda}'$ disagree decays exponentially with the sample size n , leading to an exponentially decreasing excess term.

4.2 Exact Control under Monotonicity

We now consider a stronger structural assumption on the loss function.

Proposition 3 (Exact Control under Monotonicity). *Under the assumptions of Theorem 1, suppose $L_i(\lambda)$ is non-increasing in λ and that λ_m satisfies $L_i(\lambda_m) \leq \alpha$ almost surely. Define*

$$\hat{\lambda}' = \inf \left\{ \lambda \in \Lambda : \hat{R}_{n+1}(\lambda) \leq \alpha \right\},$$

where $\hat{R}_{n+1}(\lambda) = \frac{1}{n+1} \sum_{i=1}^{n+1} L_i(\lambda)$, and let $\hat{\lambda}$ be as in Theorem 1. Then

$$\mathbb{E}[L_{n+1}(\hat{\lambda})] \leq \alpha.$$

Proof. The proof of Theorem 1 (Appendix B) establishes the decomposition

$$\mathbb{E}[L_{n+1}(\hat{\lambda})] = \mathbb{E}[L_{n+1}(\hat{\lambda}')] + \Delta_n,$$

where $\Delta_n = \mathbb{E}[L_{n+1}(\hat{\lambda})] - \mathbb{E}[L_{n+1}(\hat{\lambda}')]$. Under monotonicity, $\hat{\lambda} \geq \hat{\lambda}'$ implies $L_{n+1}(\hat{\lambda}) \leq L_{n+1}(\hat{\lambda}')$ almost surely and hence $\Delta_n \leq 0$. Moreover, $\hat{R}_{n+1}(\hat{\lambda}') \leq \alpha$ by construction, and exchangeability gives

$$\mathbb{E}[L_{n+1}(\hat{\lambda}')] = \mathbb{E}[\hat{R}_{n+1}(\hat{\lambda}')] \leq \alpha.$$

Combining the two inequalities yields $\mathbb{E}[L_{n+1}(\hat{\lambda})] \leq \alpha$. □

This argument parallels the classical proof of conformal risk control and confirms that the standard CRC guarantee holds under monotone losses in the present framework. In contrast, Theorem 1 shows that without this structural condition an excess term of order $\mathcal{O}(\sqrt{\log m/n})$ may arise.

We note that the guarantee $\mathbb{E}[L_{n+1}(\hat{\lambda})] \leq \alpha$ eliminates the statistical excess term $D(m, n)$ present in the non-monotonic case, but does not address the discretization gap discussed in Section 3.2: if the continuous oracle λ_{ora} does not belong to Λ , the grid-restricted selection may still be more conservative than optimal. In this sense, “exact” refers to the absence of statistical excess over the target level α , not to the absence of approximation error due to discretization.

Taken together, these results reveal a hierarchy of guarantees for CRC. Without structural assumptions, Theorem 1 yields an excess term of order $\mathcal{O}(\sqrt{\log m/n})$. Under Lipschitz continuity, the excess depends on the stability of the selected threshold and may decay exponentially when a margin condition holds. Finally, under monotone losses, the excess term disappears entirely, recovering exact α -level risk control.

5 Comparison with Existing Methods for Handling Non-Monotonic Loss

We compare our approach with two existing strategies for handling non-monotonic losses in conformal risk control (CRC): monotonicization techniques [Angelopoulos et al., 2024b] and stability-based methods [Angelopoulos, 2026]. Both methods aim to restore validity when the standard monotonicity assumption fails, but they differ fundamentally in their treatment of non-monotonicity.

5.1 Monotonization Techniques

Angelopoulos et al. [2024b] proposed two approaches that restore the monotonicity required by conformal risk control (CRC) by explicitly modifying either the loss function or the empirical risk. Both procedures reduce the non-monotonic setting to the standard monotone CRC framework.

Loss monotonization. Given calibration losses $\{L_i(\lambda)\}_{i=1}^n$, define

$$\tilde{L}_i(\lambda) := \sup_{t \geq \lambda} L_i(t), \quad \tilde{R}_n(\lambda) := \frac{1}{n} \sum_{i=1}^n \tilde{L}_i(\lambda).$$

The transformed losses $\tilde{L}_i(\lambda)$ are non-increasing in λ and satisfy $\tilde{L}_i(\lambda) \geq L_i(\lambda)$. Applying CRC to \tilde{R}_n yields the threshold

$$\tilde{\lambda} = \inf \left\{ \lambda : \frac{n}{n+1} \tilde{R}_n(\lambda) + \frac{B}{n+1} \leq \alpha \right\},$$

which guarantees $\mathbb{E}[L_{n+1}(\tilde{\lambda})] \leq \alpha$ with finite-sample validity. However, replacing each loss by its worst-case value over $[\lambda, \lambda_{\max}]$ can introduce substantial conservativeness, particularly when individual loss curves exhibit heterogeneous non-monotonic patterns.

Risk monotonization. Monotonicity can alternatively be imposed at the level of the empirical risk by defining

$$\hat{R}_n^\uparrow(\lambda) := \sup_{t \geq \lambda} \hat{R}_n(t), \quad \hat{\lambda}_n^\uparrow := \inf \{ \lambda : \hat{R}_n^\uparrow(\lambda) \leq \alpha \}.$$

Since aggregation precedes monotonization, this approach avoids the per-sample worst-case inflation of loss monotonization. Nevertheless, it provides only asymptotic risk control [Angelopoulos et al., 2024b, Theorem A.1].

Comparison of the two procedures. The two monotonization strategies differ in both the risk estimate and the selection criterion. For any λ ,

$$\hat{R}_n^\uparrow(\lambda) = \sup_{t \geq \lambda} \hat{R}_n(t) \leq \frac{1}{n} \sum_{i=1}^n \sup_{s \geq \lambda} L_i(s) = \tilde{R}_n(\lambda),$$

since the supremum of an average does not exceed the average of suprema. Thus risk monotonization produces a pointwise smaller risk curve. However, the two methods also use different threshold conditions: loss monotonization applies the CRC finite-sample correction (selecting where $\frac{n}{n+1}\tilde{R}_n + \frac{B}{n+1} \leq \alpha$), while risk monotonization thresholds directly at $\hat{R}_n^\dagger \leq \alpha$ without correction. Since risk monotonization operates on a smaller risk curve but at the nominal level α (rather than the effectively stricter level used by loss monotonization), it is typically less conservative in practice. The trade-off is that loss monotonization provides finite-sample validity, while risk monotonization offers only asymptotic guarantees.

In contrast, our method (Theorem 1) leaves both the loss function and the empirical risk curve unchanged. Rather than enforcing monotonicity, it treats non-monotonicity as a finite model-selection problem over the parameter grid $\Lambda = \{\lambda_1, \dots, \lambda_m\}$. The excess term $D(m, n)$ from Theorem 1 is minimax optimal (Proposition 1) and vanishes as $n \rightarrow \infty$. Exact control at level α is obtained by selecting at the adjusted level $\alpha' = \alpha - D(m, n)$.

Illustrative comparison. To compare the three approaches on equal footing, we construct a synthetic bounded loss whose population risk is non-monotonic. The per-sample loss is

$$L_i(\lambda) = s_i \cdot 0.50 e^{-8\lambda} + h_i \exp\left(-\frac{(\lambda - c_i)^2}{2\sigma_i^2}\right) + \varepsilon_i,$$

where

$$\begin{aligned} s_i &\sim \text{Unif}(0.80, 1.20), & h_i &\sim \text{Unif}(0.06, 0.20), & c_i &\sim \mathcal{N}(0.42, 0.06^2), \\ \sigma_i &\sim \text{Unif}(0.04, 0.09), & \varepsilon_i &\sim \mathcal{N}(0, 0.01^2). \end{aligned}$$

The exponential term produces a decreasing baseline risk, while the Gaussian component introduces a localized bump that temporarily pushes the risk above the target level. All losses are clipped to $[0, 1]$. We use $n = 10,000$ calibration samples, $m = 100$ candidate thresholds, and target risk level $\alpha = 0.10$. All three methods are calibrated to ensure that

$$\mathbb{E}[L_{n+1}] \leq \alpha.$$

The *loss-monotonization* (Loss mono) method selects the model using the CRC-corrected, monotone risk at level α . The *risk-monotonization* (Risk mono) method selects based on the monotone empirical risk at level α , without finite-sample correction. Our proposed method, *CRC-NM*, performs selection at the adjusted level

$$\alpha' = \alpha - D(m, n) \approx 0.085,$$

where $D(100, 10,000) \approx 0.015$.

Figure 1 shows that the empirical risk $\hat{R}_n^+(\lambda)$ violates the monotonicity assumption due to the localized bump. Both monotone strategies restore monotonicity through right-envelope

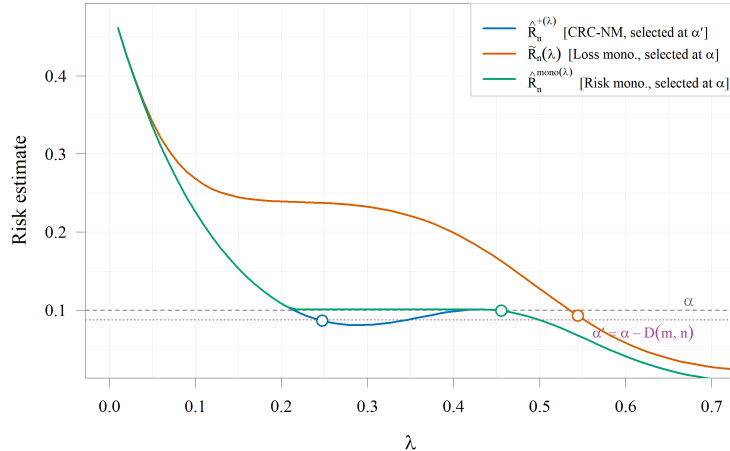


Figure 1: Empirical risk curves and selected thresholds under a non-monotonic loss ($n = 10,000$, $m = 100$, $\alpha = 0.10$). The empirical risk $\hat{R}_n^+(\lambda)$ (blue) exhibits a non-monotonic bump near $\lambda \approx 0.35$. Loss monotonicization $\tilde{R}_n^+(\lambda)$ (orange) and risk monotonicization $\hat{R}_n^{\uparrow}(\lambda)$ (green) enforce monotonicity via right-envelope corrections and select at level α (dashed grey line). CRC-NM selects at the adjusted level $\alpha' = \alpha - D(m, n)$ (dotted line). Open circles mark the selected thresholds. In this example, despite operating at a stricter level, CRC-NM selects the smallest threshold.

corrections, but at the cost of inflating the risk estimate across the parameter range. CRC-NM instead operates directly on the original risk curve and exploits the feasible region before the bump, selecting a threshold near $\lambda \approx 0.25$ where the empirical risk first falls below α' . Despite the stricter selection level, CRC-NM selects the smallest threshold in this experiment.

This behavior reflects the fundamental difference between the approaches. Monotonization incurs a *structural* cost: the right-envelope correction propagates the non-monotonic bump across smaller values of λ , preventing selection in the pre-bump feasible region. CRC-NM instead pays a *statistical* cost $D(m, n)$ that is explicit, minimax optimal, and vanishes at rate $O(\sqrt{\log m/n})$. For the parameters in this experiment, the statistical penalty ($D \approx 0.015$) is substantially smaller than the structural penalty introduced by monotonicization, resulting in a less conservative threshold selection.

5.2 Stability-Based Approaches

Another approach to handling non-monotonic losses is based on algorithmic stability [Angelopoulos, 2026]. In this framework, an algorithm \mathcal{A} maps calibration data to a parameter choice. Let $D_{1:n+1}$ denote an i.i.d. sample and D_{-i} the dataset with the i th observation removed. The algorithm is said to be β -stable with respect to an oracle procedure \mathcal{A}^* if

$$\mathbb{E} \left[\frac{1}{n+1} \sum_{i=1}^{n+1} \ell(X_i, Y_i; \mathcal{A}(D_{-i})) \right] \leq \mathbb{E} \left[\frac{1}{n+1} \sum_{i=1}^{n+1} \ell(X_i, Y_i; \mathcal{A}^*(D_{1:n+1})) \right] + \beta. \quad (4)$$

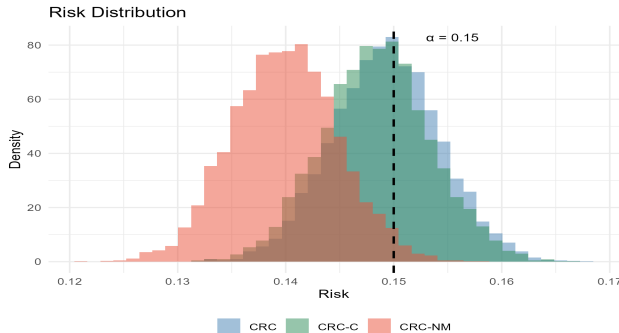


Figure 2: Risk distributions on ImageNet using ResNet-18 predictions with $n = 40,000$ calibration samples, $m = 200$ candidate thresholds, and target level $\alpha = 0.15$, averaged over 5,000 random calibration–test splits. The loss combines miscoverage with a small oversize penalty, inducing non-monotonic behavior with respect to the prediction-set threshold. CRC, CRC-C, and CRC-NM achieve similar empirical risk levels, while CRC-NM applies a larger explicit correction.

If the oracle satisfies $\mathbb{E}[\ell(X_{n+1}, Y_{n+1}; \mathcal{A}^*(D_{1:n+1}))] \leq \alpha - \beta$, then the practical algorithm achieves risk control at level α . Within this framework, standard CRC can be applied either at the nominal level α or at an adjusted level $\alpha' = \alpha - \hat{\beta}$, where $\hat{\beta}$ is obtained via bootstrap estimation. We denote the adjusted version by CRC-C.

The stability framework can yield tight guarantees when the stability constant is small and can be reliably estimated. As an illustration, for smooth losses such as the FDR in segmentation considered in Angelopoulos [2026], bootstrap estimates yield $\hat{\beta} \approx 0.00007$, so that CRC-C is nearly equivalent to standard CRC. However, bootstrap estimation requires care: using the mean of signed differences can yield $\hat{\beta} = 0$ for stable problems, necessitating the use of the 90th percentile of absolute differences as a more robust estimator.

In contrast, our result in Theorem 1 provides an explicit finite-sample bound requiring only bounded losses and a finite parameter space. The correction $D(m, n)$ depends only on observable quantities (n, m, B, α) and can be evaluated directly without stability analysis or bootstrap estimation.

Figure 2 compares CRC, CRC-C, and CRC-NM on ImageNet using ResNet-18 predictions under a non-monotonic loss function. The loss is defined as a weighted combination of miscoverage and a penalty for oversized prediction sets:

$$L(C(X; \lambda), Y) = (1 - \gamma)\mathbf{1}\{Y \notin C(X; \lambda)\} + \gamma\mathbf{1}\{|C(X; \lambda)| > K_0\},$$

with $\gamma = 0.10$ and $K_0 = 5$ (ImageNet has 1,000 classes, so this penalizes prediction sets covering more than 0.5% of the label space). Prediction sets are constructed via cumulative softmax thresholding.

As λ increases, miscoverage typically decreases, while the size of the prediction set grows. Once $|C(X; \lambda)| > K_0$, the oversize penalty is activated, resulting in a non-monotonic risk curve.

Across 5,000 random calibration–test splits, all three methods achieve empirical risks close to

the target level $\alpha = 0.15$. Standard CRC selects thresholds directly from the empirical risk curve, whereas CRC-C applies a bootstrap stability correction $\alpha' = \alpha - \hat{\beta}$, with $\hat{\beta}$ estimated from 200 bootstrap resamples. In this setting, the loss exhibits relatively low variability and the calibration sample size is large, leading to a small stability estimate and only a minor adjustment relative to CRC.

In contrast, CRC-NM employs the explicit finite-sample correction $D(m, n)$ derived in Theorem 1. This correction is typically larger than the bootstrap estimate $\hat{\beta}$, reflecting its worst-case nature: $D(m, n)$ controls the uniform deviation over all m candidate thresholds, whereas $\hat{\beta}$ captures the local stability of the selected threshold. Consequently, CRC-NM tends to select slightly more conservative thresholds, yielding marginally larger prediction sets.

Overall, this experiment highlights a regime where the loss is non-monotonic but empirically stable. In such cases, CRC-C can provide tighter, data-adaptive corrections when the bootstrap estimate is reliable, while CRC-NM offers a principled finite-sample guarantee without requiring stability assumptions or monotonicity conditions.

6 Examples

We evaluate the proposed method from Theorem 1 across several application domains. In each experiment, we compare CRC, the bootstrap-corrected variant CRC-C Angelopoulos [2026], the loss and risk monotonicity approaches (Loss Mono and Risk Mono) of Angelopoulos et al. [2024b], and the proposed CRC-NM.

All methods are implemented using the notation and settings introduced earlier. In particular, CRC and CRC-C operate at levels α and $\alpha' = \alpha - \hat{\beta}$, respectively, while CRC-NM applies the finite-sample correction from Theorem 1 directly to the non-monotone risk curve.

6.1 Synthetic multilabel experiment

We begin with a controlled multilabel classification experiment designed to induce strongly non-monotone risk curves. This setting allows us to isolate the behavior of the different procedures under pronounced violations of the monotonicity assumption.

We simulate data from a conditionally independent multilabel logistic model. Each observation consists of a feature vector $X \in \mathbb{R}^d$ and a binary label vector $Y = (Y_1, \dots, Y_K) \in \{0, 1\}^K$, where $Y_k \in \{0, 1\}$ indicates whether label k is present. Features are drawn as $X \sim \mathcal{N}(0, I_d)$ with $d = 15$, and

$$\Pr(Y_k = 1 \mid X) = \sigma(X^\top W_k + b_k),$$

where $\sigma(z) = 1/(1 + e^{-z})$, $W_k \sim \mathcal{N}(0, 0.8^2 I_d)$, and $b_k \sim \mathcal{N}(0, 0.2^2)$. Labels are sampled independently across k given X .

Predicted probabilities are constructed by adding Gaussian noise to the logits prior to applying the sigmoid transformation, yielding imperfect probability estimates. Prediction sets are defined

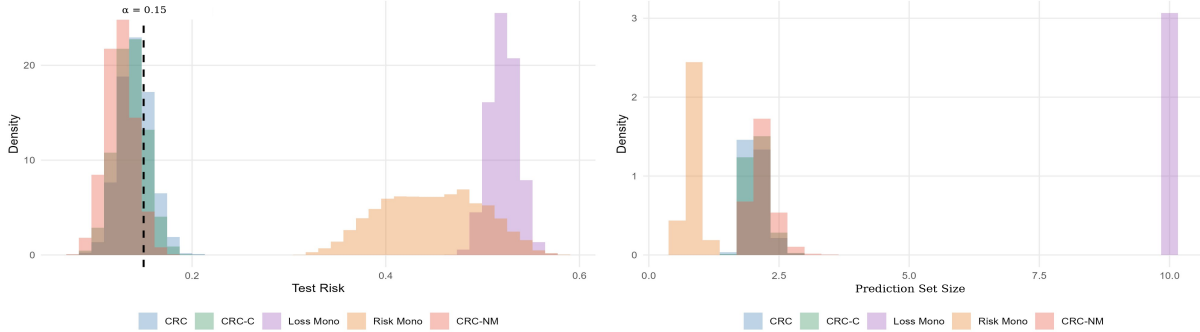


Figure 3: Synthetic multilabel experiment based on 1,000 repetitions. Left: distribution of test risks; the dashed line indicates the target level $\alpha = 0.15$. Loss and risk monotonicization select extreme thresholds when the monotonicized risk exceeds α across the entire grid, resulting in test risks far above the target. Right: distribution of prediction set sizes across methods.

as

$$C(X; \lambda) = \{k : \hat{p}_k(X) \geq 1 - \lambda\}.$$

To induce non-monotonicity, we consider a precision-based loss

$$L(X, Y; \lambda) = \ell\left(\frac{|Y \cap C(X; \lambda)|}{|C(X; \lambda)|}\right), \quad \ell(x) = 1 - x + 0.22 \sin(2\pi x)(1 - x).$$

The ratio $|Y \cap C|/|C|$ corresponds to the precision of the prediction set. While enlarging the set improves recall, it may reduce precision; the sinusoidal modulation accentuates this trade-off, ensuring that the loss is highly non-monotone in λ . The resulting risk curve exhibits oscillations with amplitude approximately 0.04–0.06, which is substantial relative to the target level $\alpha = 0.15$ (roughly one-third of α).

We use $K = 10$ labels, $n_{\text{cal}} = 10,000$ calibration samples, and $n_{\text{test}} = 500$ test samples. The target risk level is $\alpha = 0.15$, and the threshold grid contains $m = 100$ candidate values. Results are averaged over 1,000 independent repetitions.

Figure 3 summarizes the results. The left panel shows the distribution of test risks, while the right panel shows the corresponding prediction-set sizes. CRC, CRC-C, and CRC-NM all achieve empirical risks close to the target level, with CRC-C and CRC-NM producing slightly larger sets.

The monotonicization procedures behave markedly differently. Because the full prediction set incurs relatively high loss under the precision-based criterion, the supremum operations used in these methods propagate this value across the threshold grid. Consequently, the monotonicized risk curve can exceed α uniformly, leaving no feasible thresholds and forcing selection at extreme values.

Overall, this experiment highlights a regime in which strong non-monotonicity causes monotonicization-based approaches to break down. In contrast, CRC-NM maintains stable risk control while operating directly on the original risk curve, without requiring transformations of the loss or monotonicity assumptions.

6.2 COCO object detection

We evaluate the proposed methods on a real-data object detection problem using the COCO 2017 validation set. A pretrained Faster R-CNN detector with a ResNet-50-FPN backbone is used to generate candidate detections. We randomly sample 3,000 images from the validation set for analysis.

For each image X , the detector produces a set of candidate bounding boxes with associated confidence scores. Given a parameter $\lambda \in [0, 1]$, we define the prediction set $C(X; \lambda)$ as the collection of detections with confidence score at least $t = 1 - \lambda$. Thus, increasing λ lowers the score threshold and yields larger prediction sets.

To compare detections with ground truth, we perform greedy bipartite matching using an intersection-over-union (IoU) threshold of 0.3. This relatively permissive threshold emphasizes detection performance rather than precise localization. Let n_{matched} denote the number of matched detections, n_{gt} the number of ground-truth boxes, and $|C(X; \lambda)|$ the size of the prediction set.

For each image (X, Y) , we define the loss

$$L(X, Y; \lambda) = (1 - \gamma) \left(1 - \frac{n_{\text{matched}}}{n_{\text{gt}}} \right) + \gamma \phi(|C(X; \lambda)|),$$

where

$$\phi(s) = \min\left(\frac{(s - K_0)_+}{\tau}, 1\right).$$

In our experiments, we set $\gamma = 0.35$, $K_0 = 3$, and $\tau = 5$. The first term represents a recall-type error, while the second term penalizes large prediction sets.

As λ increases, the score threshold decreases, leading to more detections. The miss term is therefore non-increasing in λ , whereas the penalty term is non-decreasing once $|C(X; \lambda)| > K_0$. Consequently, the loss $L(X, Y; \lambda)$ is generally non-monotone in λ .

We consider a grid of $m = 200$ values of λ uniformly spaced in $[0.02, 0.75]$. For each repetition, the data are randomly split into a calibration set of size $n_{\text{cal}} = 2,500$ and a test set of size $n_{\text{test}} = 800$. The target risk level is $\alpha = 0.33$. All results are obtained by averaging over 3,000 independent random calibration–test splits.

For CRC-C, the stability correction $\hat{\beta}$ is estimated as the empirical 90th percentile of absolute bootstrap risk deviations based on 200 bootstrap resamples. CRC-NM uses the explicit finite-sample correction $D(m, n)$ from Theorem 1.

The empirical risk curve exhibits non-monotonic behavior, with the minimum attained in the interior of the parameter grid. Figure 4 summarizes the results. The left panel shows the distribution of test risks across repeated splits, and the right panel shows the corresponding distribution of prediction-set sizes.

Standard CRC and risk monotonization select relatively small prediction sets and produce empirical risks close to the target level. CRC-C behaves similarly, indicating that the estimated

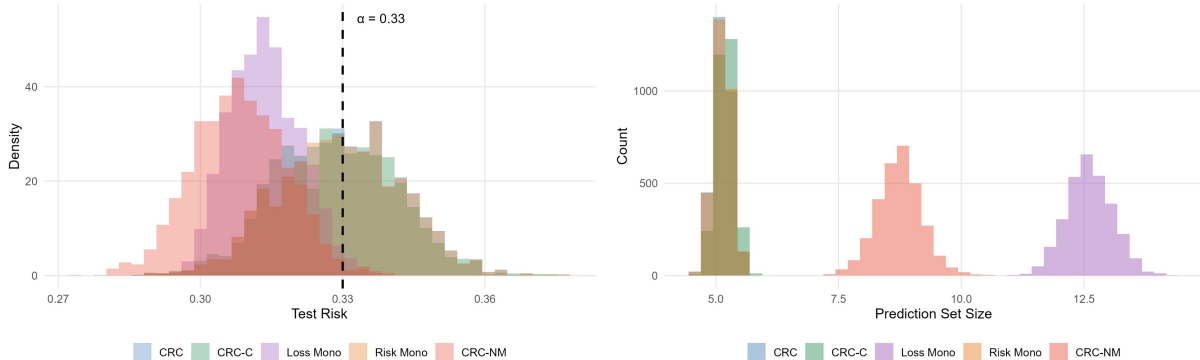


Figure 4: COCO object detection experiment. Left: distribution of test risks across repeated calibration–test splits; the dashed line indicates the target risk level $\alpha = 0.33$. Right: distribution of prediction-set sizes for each method.

stability correction is small in this setting. In contrast, CRC-NM selects moderately larger prediction sets and yields empirical risks that are typically below the target level, reflecting its explicit finite-sample correction. The loss-monotonization approach is the most conservative, producing the largest prediction sets and the lowest risks among the methods considered.

Differences in violation rates are also observed. Due to the non-monotonicity of the loss, standard CRC and risk monotization frequently exceed the target level across repeated splits. CRC-C provides only modest improvement. In contrast, CRC-NM substantially reduces violations while remaining less conservative than loss monotization.

Overall, these results are consistent with the theoretical guarantees of CRC-NM, indicating improved control of the target risk level under non-monotone losses without requiring transformation of the loss function or risk curve.

These experiments illustrate that non-monotonicity can substantially affect the behavior of conformal risk control procedures, and that explicit finite-sample correction is effective in stabilizing risk control in such settings.

7 Extensions

We extend our framework to settings with *distributional shift*, where the distribution generating the calibration data differs from the distribution under which the prediction procedure is deployed. Such situations arise frequently in practice when the training data is collected under historical conditions, while predictions are evaluated under a different population or environment.

Let $(X_1, Y_1), \dots, (X_n, Y_n)$ be i.i.d. observations from the training distribution P_{train} , and let (X_{n+1}, Y_{n+1}) be drawn from the test distribution P_{test} . We assume that P_{test} is absolutely continuous with respect to P_{train} , denoted $P_{\text{test}} \ll P_{\text{train}}$, with likelihood ratio

$$w(x, y) = \frac{dP_{\text{test}}}{dP_{\text{train}}}(x, y).$$

To control the variance of importance-weighted quantities, we assume that the likelihood ratio is bounded:

$$0 \leq w(x, y) \leq W < \infty.$$

This assumption is standard in analyses based on importance weighting and ensures that weighted losses remain bounded, allowing concentration inequalities to be applied. In practice, boundedness can often be enforced through weight truncation.

Under this assumption, expectations under the test distribution can be expressed using importance weighting. Specifically, for any measurable function g ,

$$\mathbb{E}_{P_{\text{test}}}[g(X, Y)] = \mathbb{E}_{P_{\text{train}}}[w(X, Y) g(X, Y)].$$

This identity allows us to estimate the test risk using training data by reweighting observations according to the likelihood ratio.

Proposition 4 (Distributional shift). *Assume $0 \leq L(X, Y; \lambda) \leq B$ almost surely for all $\lambda \in \Lambda = \{\lambda_1, \dots, \lambda_m\}$. Define the test risk*

$$R_{\text{test}}(\lambda) = \mathbb{E}_{P_{\text{test}}}[L(X, Y; \lambda)].$$

Let the weighted losses be

$$L_i^w(\lambda) = w(X_i, Y_i)L(X_i, Y_i; \lambda),$$

which satisfy $0 \leq L_i^w(\lambda) \leq WB$. Define the weighted empirical risk

$$\hat{R}_n^w(\lambda) = \frac{1}{n} \sum_{i=1}^n L_i^w(\lambda).$$

Define

$$\hat{\lambda} = \inf \left\{ \lambda \in \Lambda : \frac{n}{n+1} \hat{R}_n^w(\lambda) + \frac{WB}{n+1} \leq \alpha \right\},$$

with $\inf \emptyset = \lambda_m$.

If there exists $\lambda^* \in \Lambda$ such that

$$R_{\text{test}}(\lambda^*) \leq \alpha,$$

then

$$\mathbb{E} \left[L(X_{n+1}, Y_{n+1}; \hat{\lambda}) \right] \leq \alpha + WB \sqrt{\frac{\log(2m)}{2n}} + \frac{WB}{2\sqrt{2n \log(2m)}},$$

where the expectation is taken over $(X_{1:n}, Y_{1:n}) \sim P_{\text{train}}^n$ and $(X_{n+1}, Y_{n+1}) \sim P_{\text{test}}$.

Proposition 4 shows that the finite-sample guarantee established in the i.i.d. setting extends naturally to the distribution-shift scenario. The only modification required is replacing the empirical risk with its importance-weighted counterpart. The resulting excess term scales linearly with the bound W on the likelihood ratio, reflecting the increased variability introduced by importance weighting.

Special case: covariate shift. An important special case occurs when the conditional distribution of the response remains unchanged:

$$P_{\text{test}}(Y | X) = P_{\text{train}}(Y | X).$$

This setting is commonly referred to as *covariate shift*. In this case the likelihood ratio depends only on the feature vector:

$$w(x, y) = w(x) = \frac{dP_{\text{test}}(x)}{dP_{\text{train}}(x)}.$$

Thus covariate shift is a special case of Proposition 4. The estimator and theoretical guarantee remain identical; the only difference is that practitioners estimate a marginal density ratio $w(x)$ rather than the joint ratio $w(x, y)$.

Remark. The excess term grows linearly with W , reflecting the additional variability introduced by importance weighting and an effective reduction in the usable sample size under distributional shift. When W is large, more calibration data may be required to maintain accurate risk control. Handling unbounded or heavy-tailed likelihood ratios would require additional techniques, such as weight truncation or robust importance-weighting methods, which are beyond the scope of this work.

8 Conclusion

We extend conformal risk control to bounded, non-monotone loss functions over discrete parameter grids. Our results show that monotonicity is not required for finite-sample expectation control: the excess risk induced by parameter selection grows only logarithmically with the grid size and vanishes as the calibration sample size increases. This provides a simple and general framework for controlling predictive risk even when the loss function does not satisfy the structural assumptions typically imposed by existing CRC methods.

From a conceptual perspective, our analysis shows that non-monotonicity can be addressed by viewing parameter selection as a statistical model-selection problem over a finite grid. Rather than enforcing monotonicity or imposing algorithmic stability conditions, we directly control the excess risk introduced by searching over candidate parameters. This perspective yields explicit finite-sample guarantees that hold for arbitrary bounded loss functions without requiring monotonicity.

These guarantees broaden the applicability of conformal risk control to settings where loss functions are inherently non-monotone. Such situations arise, for example, when a tuning parameter governs a discrete decision rule or classification threshold, where small changes in the parameter can lead to abrupt changes in predictions. Several directions for future work remain open, including extending the analysis to continuous parameter spaces, handling heavy-tailed or unbounded loss functions, and obtaining sharper bounds under additional structural assumptions.

Overall, our results demonstrate that reliable conformal risk control can be achieved without monotonicity assumptions, requiring only bounded losses and a finite parameter grid.

A Lemmas

Lemma 1 (Uniform Concentration Bound). *Let $L_1(\lambda), \dots, L_n(\lambda)$ be i.i.d. random variables with $L_i(\lambda) \in [0, B]$ for all $\lambda \in \Lambda = \{\lambda_1, \dots, \lambda_m\}$. Define the empirical risk $\hat{R}_n(\lambda) = \frac{1}{n} \sum_{i=1}^n L_i(\lambda)$ and the true risk $R(\lambda) = \mathbb{E}[L_i(\lambda)]$. Then*

$$\mathbb{E} \left[\sup_{\lambda \in \Lambda} \left| \hat{R}_n(\lambda) - R(\lambda) \right| \right] \leq B \sqrt{\frac{\log(2m)}{2n}} + \frac{B}{2\sqrt{2n \log(2m)}}.$$

Proof. Define $Z = \sup_{\lambda \in \Lambda} |\hat{R}_n(\lambda) - R(\lambda)|$. By Hoeffding's inequality, for any fixed $\lambda \in \Lambda$ and $t > 0$,

$$\mathbb{P} \left(|\hat{R}_n(\lambda) - R(\lambda)| \geq t \right) \leq 2 \exp \left(-\frac{2nt^2}{B^2} \right).$$

Applying the union bound over Λ ,

$$\mathbb{P}(Z \geq t) \leq 2m \exp \left(-\frac{2nt^2}{B^2} \right). \quad (5)$$

Since $Z \leq B$ almost surely, we write

$$\mathbb{E}[Z] = \int_0^B \mathbb{P}(Z \geq t) dt.$$

Define $t^* = B \sqrt{\frac{\log(2m)}{2n}}$, chosen so that the tail bound (5) equals 1 at $t = t^*$:

$$2m \exp \left(-\frac{2n(t^*)^2}{B^2} \right) = 2m \exp(-\log(2m)) = 1.$$

We split the integral at t^* :

$$\mathbb{E}[Z] = \int_0^{t^*} \mathbb{P}(Z \geq t) dt + \int_{t^*}^B \mathbb{P}(Z \geq t) dt.$$

For the first integral, $\mathbb{P}(Z \geq t) \leq 1$, so

$$\int_0^{t^*} \mathbb{P}(Z \geq t) dt \leq t^* = B \sqrt{\frac{\log(2m)}{2n}}.$$

For the second integral, we apply (5):

$$\int_{t^*}^B \mathbb{P}(Z \geq t) dt \leq \int_{t^*}^{\infty} 2m \exp \left(-\frac{2nt^2}{B^2} \right) dt.$$

Substituting $u = t\sqrt{2n}/B$ (so $dt = B du/\sqrt{2n}$) with $u^* = t^*\sqrt{2n}/B = \sqrt{\log(2m)}$,

$$\int_{t^*}^{\infty} 2m \exp\left(-\frac{2nt^2}{B^2}\right) dt = \frac{2mB}{\sqrt{2n}} \int_{u^*}^{\infty} e^{-u^2} du.$$

Using the Gaussian tail bound $\int_v^{\infty} e^{-u^2} du \leq \frac{e^{-v^2}}{2v}$ for $v > 0$,

$$\int_{u^*}^{\infty} e^{-u^2} du \leq \frac{e^{-(u^*)^2}}{2u^*} = \frac{e^{-\log(2m)}}{2\sqrt{\log(2m)}} = \frac{1}{4m\sqrt{\log(2m)}}.$$

Therefore,

$$\int_{t^*}^B \mathbb{P}(Z \geq t) dt \leq \frac{2mB}{\sqrt{2n}} \cdot \frac{1}{4m\sqrt{\log(2m)}} = \frac{B}{2\sqrt{2n \log(2m)}}.$$

Combining both parts:

$$\mathbb{E}[Z] \leq B\sqrt{\frac{\log(2m)}{2n}} + \frac{B}{2\sqrt{2n \log(2m)}}.$$

□

B Proofs

B.1 Proof of Theorem 1

Proof. Let $\Lambda = \{\lambda_1, \dots, \lambda_m\}$ with $\lambda_1 < \dots < \lambda_m$. Define

$$\hat{R}_{n+1}(\lambda) = \frac{1}{n+1} \sum_{i=1}^{n+1} L_i(\lambda),$$

and let

$$\hat{\lambda}' = \inf\{\lambda \in \Lambda : \hat{R}_{n+1}(\lambda) \leq \alpha\}, \quad \hat{\lambda} = \inf\left\{\lambda \in \Lambda : \frac{n}{n+1} \hat{R}_n(\lambda) + \frac{B}{n+1} \leq \alpha\right\},$$

with $\inf \emptyset = \lambda_m$ in both cases.

Step 1: $\hat{\lambda}' \leq \hat{\lambda}$ **a.s.** If λ is feasible for $\hat{\lambda}$, then

$$\hat{R}_{n+1}(\lambda) = \frac{n}{n+1} \hat{R}_n(\lambda) + \frac{L_{n+1}(\lambda)}{n+1} \leq \frac{n}{n+1} \hat{R}_n(\lambda) + \frac{B}{n+1} \leq \alpha,$$

so λ is also feasible for $\hat{\lambda}'$. Hence the feasible set for $\hat{\lambda}'$ contains that for $\hat{\lambda}$, giving $\hat{\lambda}' \leq \hat{\lambda}$. If neither feasible set is nonempty, both default to λ_m and equality holds.

Step 2: $\mathbb{E}[L_{n+1}(\hat{\lambda}')] \leq \alpha$. Since L_1, \dots, L_{n+1} are i.i.d., they are exchangeable. Hence $\mathbb{E}[L_i(\hat{\lambda}')] is the same for every $i \in [n+1]$, and in particular$

$$\mathbb{E}[L_{n+1}(\hat{\lambda}')] = \frac{1}{n+1} \sum_{i=1}^{n+1} \mathbb{E}[L_i(\hat{\lambda}')] = \mathbb{E}[\hat{R}_{n+1}(\hat{\lambda}')].$$

When the feasible set for $\hat{\lambda}'$ is nonempty, $\hat{R}_{n+1}(\hat{\lambda}') \leq \alpha$ by construction. When it is empty, $\hat{\lambda}' = \lambda_m$ by convention. By assumption, there exists $\lambda^* \in \Lambda$ with $R(\lambda^*) \leq \alpha$. The event that the feasible set is empty requires $\hat{R}_{n+1}(\lambda^*) > \alpha$, i.e., $\hat{R}_{n+1}(\lambda^*) - R(\lambda^*) > \alpha - R(\lambda^*) \geq 0$. On this event, $\hat{R}_{n+1}(\hat{\lambda}') \leq B$. Therefore

$$\begin{aligned} \mathbb{E}[\hat{R}_{n+1}(\hat{\lambda}')] &= \mathbb{E}[\hat{R}_{n+1}(\hat{\lambda}') \mathbf{1}\{\text{feasible set nonempty}\}] + \mathbb{E}[\hat{R}_{n+1}(\hat{\lambda}') \mathbf{1}\{\text{feasible set empty}\}] \\ &\leq \alpha + B \mathbb{P}(\text{feasible set empty}). \end{aligned}$$

By Hoeffding's inequality,

$$\mathbb{P}(\text{feasible set empty}) \leq \mathbb{P}(\hat{R}_{n+1}(\lambda^*) > \alpha) \leq \exp\left(-\frac{2(n+1)(\alpha - R(\lambda^*))^2}{B^2}\right).$$

This probability decays exponentially and is absorbed into the leading $\mathcal{O}(\sqrt{\log m/n})$ term in the final bound. More precisely, the contribution $B \exp(-2(n+1)(\alpha - R(\lambda^*))^2/B^2)$ is at most $B\sqrt{\log(2m)/(2n)}$ for n satisfying $(\alpha - R(\lambda^*))^2 \geq B^2 \log(2m)/(4n)$, which holds whenever n is large enough that the bound in the theorem is nontrivial. We thus have

$$\mathbb{E}[L_{n+1}(\hat{\lambda}')] \leq \alpha + o_n(1),$$

where the residual is dominated by the uniform concentration term below.

Step 3: Three-term decomposition. Define $\Delta_n = \mathbb{E}[L_{n+1}(\hat{\lambda})] - \mathbb{E}[L_{n+1}(\hat{\lambda}')]$. Since $\hat{\lambda}$ is measurable with respect to (L_1, \dots, L_n) and L_{n+1} is independent of these,

$$\mathbb{E}[L_{n+1}(\hat{\lambda})] = \mathbb{E}[R(\hat{\lambda})].$$

Decompose Δ_n as

$$\Delta_n = \underbrace{\mathbb{E}[R(\hat{\lambda}) - \hat{R}_n(\hat{\lambda})]}_{(I)} + \underbrace{\mathbb{E}[\hat{R}_n(\hat{\lambda}) - \hat{R}_n(\hat{\lambda}')] }_{(II)} + \underbrace{\mathbb{E}[\hat{R}_n(\hat{\lambda}') - L_{n+1}(\hat{\lambda}')] }_{(III)}.$$

Term (I). Since $\hat{\lambda} \in \Lambda$,

$$R(\hat{\lambda}) - \hat{R}_n(\hat{\lambda}) \leq \sup_{\lambda \in \Lambda} |R(\lambda) - \hat{R}_n(\lambda)|,$$

so by Lemma 1,

$$(I) \leq B \sqrt{\frac{\log(2m)}{2n}} + \frac{B}{2\sqrt{2n \log(2m)}}.$$

Term (II). Write

$$\hat{R}_n(\hat{\lambda}) - \hat{R}_n(\hat{\lambda}') = \sum_{j=1}^m \sum_{k=1}^j (\hat{R}_n(\lambda_j) - \hat{R}_n(\lambda_k)) \mathbf{1}\{\hat{\lambda} = \lambda_j, \hat{\lambda}' = \lambda_k\}.$$

For $k < j$: $\hat{\lambda} = \lambda_j$ means λ_j is the smallest element satisfying the calibration condition, so every smaller λ_k ($k < j$) fails it, i.e., $\frac{n}{n+1}\hat{R}_n(\lambda_k) + \frac{B}{n+1} > \alpha$. Since λ_j satisfies the condition, $\frac{n}{n+1}\hat{R}_n(\lambda_j) + \frac{B}{n+1} \leq \alpha$, giving $\hat{R}_n(\lambda_j) < \hat{R}_n(\lambda_k)$. For $k = j$: the contribution is zero. Hence $(II) \leq 0$.

Term (III). By exchangeability (i.i.d. symmetry), $\mathbb{E}[L_i(\hat{\lambda}')] is the same for all $i \in [n+1]$. Therefore$

$$\mathbb{E}[\hat{R}_n(\hat{\lambda}')] = \frac{1}{n} \sum_{i=1}^n \mathbb{E}[L_i(\hat{\lambda}')] = \mathbb{E}[L_{n+1}(\hat{\lambda}')],$$

so $(III) = 0$.

Step 4: Combining. Collecting the three terms,

$$\Delta_n \leq B \sqrt{\frac{\log(2m)}{2n}} + \frac{B}{2\sqrt{2n \log(2m)}}.$$

Since $\mathbb{E}[L_{n+1}(\hat{\lambda}')] \leq \alpha$ (from Step 2, with the exponential residual absorbed),

$$\mathbb{E}[L_{n+1}(\hat{\lambda})] = \mathbb{E}[L_{n+1}(\hat{\lambda}')] + \Delta_n \leq \alpha + B \sqrt{\frac{\log(2m)}{2n}} + \frac{B}{2\sqrt{2n \log(2m)}}. \quad \square$$

B.2 Proof of Proposition 1

Proof. Fix $n \geq 1$ and $m \geq 4$, and let $\Lambda = \{\lambda_1, \dots, \lambda_m\}$. Let $\delta > 0$ be chosen later, set $p = \alpha + \delta$, and assume $\delta \leq (1 - \alpha)/2$ so that $p \in (0, 1)$.

For each $j \in [m]$, define a distribution P_j on $L = (L(\lambda_1), \dots, L(\lambda_m)) \in \{0, 1\}^m$ by taking coordinates independent with

$$L(\lambda_j) \sim \text{Bern}(\alpha), \quad L(\lambda_k) \sim \text{Bern}(p) \quad (k \neq j).$$

Let $D_{1:n} = (L_1, \dots, L_n)$ with $L_i \stackrel{\text{i.i.d.}}{\sim} P_j$ and let L_{n+1} be an independent test draw from the same P_j . Then

$$\mathbb{E}_{P_j}[L_{n+1}(\hat{\lambda})] = \alpha + \delta \mathbb{P}_{P_j}(\hat{\lambda} \neq \lambda_j). \quad (6)$$

KL bound. For $a \neq b$, the one-sample KL divergence satisfies

$$\text{KL}(P_a \| P_b) = \text{KL}(\text{Bern}(\alpha) \| \text{Bern}(p)) + \text{KL}(\text{Bern}(p) \| \text{Bern}(\alpha)).$$

By the standard quadratic bound for Bernoulli KL (see, e.g., Tsybakov [2009]), there exists a universal constant C_0 such that

$$\text{KL}(P_a \| P_b) \leq C_0 \frac{\delta^2}{\alpha(1-\alpha)}.$$

Therefore, for n i.i.d. samples,

$$\text{KL}(P_a^{\otimes n} \| P_b^{\otimes n}) = n \text{KL}(P_a \| P_b) \leq C_1 n \delta^2$$

for a universal constant C_1 .

Fano's inequality. Let $J \sim \text{Unif}([m])$ and draw $D_{1:n} \sim P_J^{\otimes n}$. By Fano's inequality (see, e.g., Tsybakov [2009]),

$$\mathbb{P}(\hat{\lambda} \neq \lambda_J) \geq 1 - \frac{I(J; D_{1:n}) + \log 2}{\log m}.$$

Moreover, the mutual information satisfies (see, e.g., Tsybakov [2009])

$$I(J; D_{1:n}) \leq \max_{a \neq b} \text{KL}(P_a^{\otimes n} \| P_b^{\otimes n}) \leq C_1 n \delta^2.$$

Hence

$$\mathbb{P}(\hat{\lambda} \neq \lambda_J) \geq 1 - \frac{C_1 n \delta^2 + \log 2}{\log m}.$$

Choose $\delta = c' \sqrt{\frac{\log m}{n}}$ with $c' > 0$ small enough so that $C_1 c'^2 \leq 1/4$ and $\delta \leq (1-\alpha)/2$. Then $C_1 n \delta^2 \leq \frac{1}{4} \log m$, and since $m \geq 4$ we have $\log 2 / \log m \leq 1/2$, yielding

$$\mathbb{P}(\hat{\lambda} \neq \lambda_J) \geq \frac{1}{4}.$$

Because J is uniform,

$$\mathbb{P}(\hat{\lambda} \neq \lambda_J) = \frac{1}{m} \sum_{j=1}^m \mathbb{P}_{P_j}(\hat{\lambda} \neq \lambda_j),$$

so there exists $j^* \in [m]$ such that $\mathbb{P}_{P_{j^*}}(\hat{\lambda} \neq \lambda_{j^*}) \geq \frac{1}{4}$. Plugging into (6) gives

$$\mathbb{E}_{P_{j^*}}[L_{n+1}(\hat{\lambda})] \geq \alpha + \frac{1}{4}\delta = \alpha + c \sqrt{\frac{\log m}{n}},$$

with $c = c'/4$. □

B.3 Proof of Proposition 2

We begin by bounding the probability that the two thresholds $\hat{\lambda}$ and $\hat{\lambda}'$ disagree.

Lemma 2 (Probability of Threshold Disagreement). *Suppose the assumptions of Theorem 1 hold. Assume there exist $\lambda^* \in \Lambda$ and $\epsilon > 0$ such that*

$$R(\lambda^*) \leq \alpha - \epsilon.$$

If $\epsilon \geq (B - \alpha)/n$, then

$$\mathbb{P}(\hat{\lambda} \neq \hat{\lambda}') \leq \exp\left(-\frac{2n\epsilon^2}{B^2}\right).$$

Proof. From Step 1 in the proof of Theorem 1, we have $\hat{\lambda}' \leq \hat{\lambda}$ almost surely. Hence

$$\{\hat{\lambda} \neq \hat{\lambda}'\} = \{\hat{\lambda} > \hat{\lambda}'\} \subseteq \{\hat{\lambda} > \lambda^*\}.$$

If λ^* is feasible for $\hat{\lambda}$, then by definition of the infimum we must have $\hat{\lambda} \leq \lambda^*$. Therefore

$$\{\hat{\lambda} > \lambda^*\} \subseteq \{\lambda^* \text{ is infeasible for } \hat{\lambda}\}.$$

Infeasibility of λ^* corresponds to the event

$$\frac{n}{n+1}\hat{R}_n(\lambda^*) + \frac{B}{n+1} > \alpha \iff \hat{R}_n(\lambda^*) > \alpha - \frac{B-\alpha}{n}.$$

If $\epsilon \geq (B - \alpha)/n$, then

$$\alpha - \frac{B-\alpha}{n} \geq \alpha - \epsilon,$$

and hence

$$\left\{\hat{R}_n(\lambda^*) > \alpha - \frac{B-\alpha}{n}\right\} \subseteq \{\hat{R}_n(\lambda^*) > \alpha - \epsilon\}.$$

Combining these relations gives

$$\mathbb{P}(\hat{\lambda} \neq \hat{\lambda}') \leq \mathbb{P}\left(\hat{R}_n(\lambda^*) > \alpha - \epsilon\right).$$

Since $R(\lambda^*) \leq \alpha - \epsilon$, the above event implies

$$\hat{R}_n(\lambda^*) - R(\lambda^*) \geq \epsilon.$$

Because $L_i(\lambda^*) \in [0, B]$ are i.i.d., Hoeffding's inequality yields

$$\mathbb{P}\left(\hat{R}_n(\lambda^*) - R(\lambda^*) \geq \epsilon\right) \leq \exp\left(-\frac{2n\epsilon^2}{B^2}\right),$$

which proves the lemma. □

Proof of Proposition 2. Recall the decomposition

$$\mathbb{E}[L_{n+1}(\hat{\lambda})] = \mathbb{E}[L_{n+1}(\hat{\lambda}')] + \Delta_n, \quad \Delta_n = \mathbb{E}\left[L_{n+1}(\hat{\lambda}) - L_{n+1}(\hat{\lambda}')\right].$$

By the K -Lipschitz property of $L_{n+1}(\cdot)$,

$$|L_{n+1}(\hat{\lambda}) - L_{n+1}(\hat{\lambda}')| \leq K |\hat{\lambda} - \hat{\lambda}'| \quad \text{a.s.}$$

Therefore

$$\Delta_n \leq K \mathbb{E}\left[|\hat{\lambda} - \hat{\lambda}'|\right].$$

Since $\hat{\lambda}, \hat{\lambda}' \in \Lambda \subseteq [\lambda_1, \lambda_m]$,

$$|\hat{\lambda} - \hat{\lambda}'| \leq \text{diam}(\Lambda) \mathbf{1}\{\hat{\lambda} \neq \hat{\lambda}'\} \quad \text{a.s.},$$

where $\text{diam}(\Lambda) = \lambda_m - \lambda_1$. Taking expectations yields

$$\Delta_n \leq K \text{diam}(\Lambda) \mathbb{P}(\hat{\lambda} \neq \hat{\lambda}').$$

Next we bound $\mathbb{E}[L_{n+1}(\hat{\lambda}')]$. Recall that

$$\hat{\lambda}' = \inf\{\lambda \in \Lambda : \hat{R}_{n+1}(\lambda) \leq \alpha\}, \quad \inf \emptyset = \lambda_m.$$

Thus $\hat{\lambda}'$ is always well defined. On the event that the feasible set $\{\lambda \in \Lambda : \hat{R}_{n+1}(\lambda) \leq \alpha\}$ is nonempty, we have $\hat{R}_{n+1}(\hat{\lambda}') \leq \alpha$.

Since $\hat{R}_{n+1}(\cdot)$ is symmetric in the sample indices, exchangeability implies

$$\mathbb{E}[L_{n+1}(\hat{\lambda}')] = \mathbb{E}[\hat{R}_{n+1}(\hat{\lambda}')] \leq \alpha.$$

Combining the above bounds gives

$$\mathbb{E}[L_{n+1}(\hat{\lambda})] \leq \alpha + K \text{diam}(\Lambda) \mathbb{P}(\hat{\lambda} \neq \hat{\lambda}').$$

The exponential refinement follows by applying Lemma 2. □

B.4 Proof of Proposition 4

Proof. Fix any $\lambda \in \Lambda$. Define the weighted loss

$$L^w(X, Y; \lambda) := w(X, Y)L(X, Y; \lambda), \quad L_i^w(\lambda) := L^w(X_i, Y_i; \lambda).$$

Since $(X_i, Y_i)_{i=1}^n$ are i.i.d. under P_{train} and $w(\cdot, \cdot)L(\cdot, \cdot; \lambda)$ is measurable, the random variables $L_1^w(\lambda), \dots, L_n^w(\lambda)$ are i.i.d. under P_{train} for each fixed λ . Moreover, using $0 \leq L \leq B$ and $0 \leq w \leq W$,

$$0 \leq L_i^w(\lambda) \leq WB \quad \text{a.s. for all } \lambda \in \Lambda.$$

Step 1: Change of measure (unconditional). Because $P_{\text{test}} \ll P_{\text{train}}$ with Radon–Nikodym derivative $w = dP_{\text{test}}/dP_{\text{train}}$, for any integrable measurable function g ,

$$\mathbb{E}_{P_{\text{test}}}[g(X, Y)] = \mathbb{E}_{P_{\text{train}}}[w(X, Y)g(X, Y)].$$

Applying this with $g(X, Y) = L(X, Y; \lambda)$ yields

$$R_{\text{test}}(\lambda) = \mathbb{E}_{P_{\text{test}}}[L(X, Y; \lambda)] = \mathbb{E}_{P_{\text{train}}}[L^w(X, Y; \lambda)].$$

Hence the feasibility assumption $R_{\text{test}}(\lambda^*) \leq \alpha$ is equivalent to

$$\mathbb{E}_{P_{\text{train}}}[L^w(X, Y; \lambda^*)] \leq \alpha.$$

Step 2: Apply Theorem 1 to the weighted problem. Consider the learning problem under P_{train} with bounded losses $L_i^w(\lambda) \in [0, WB]$ over the finite grid Λ and define

$$\hat{R}_n^w(\lambda) = \frac{1}{n} \sum_{i=1}^n L_i^w(\lambda), \quad \hat{\lambda} = \inf \left\{ \lambda \in \Lambda : \frac{n}{n+1} \hat{R}_n^w(\lambda) + \frac{WB}{n+1} \leq \alpha \right\},$$

with $\inf \emptyset = \lambda_m$. By Theorem 1, applied to the bounded losses $L_i^w(\lambda) \in [0, WB]$, we obtain

$$\mathbb{E}_{P_{\text{train}}^{n+1}} \left[L^w(X_{n+1}, Y_{n+1}; \hat{\lambda}) \right] \leq \alpha + WB \sqrt{\frac{\log(2m)}{2n}} + \frac{WB}{2\sqrt{2n \log(2m)}}.$$

Using the tower property of conditional expectation and the fact that $\hat{\lambda}$ is measurable with respect to $\sigma(X_{1:n}, Y_{1:n})$, this can be written equivalently as

$$\begin{aligned} \mathbb{E}_{P_{\text{train}}^n} \left[\mathbb{E}_{P_{\text{train}}} \left[w(X_{n+1}, Y_{n+1}) L(X_{n+1}, Y_{n+1}; \hat{\lambda}) \mid X_{1:n}, Y_{1:n} \right] \right] \\ \leq \alpha + WB \sqrt{\frac{\log(2m)}{2n}} + \frac{WB}{2\sqrt{2n \log(2m)}}. \end{aligned} \quad (7)$$

Step 3: Convert weighted train-expectation to test-expectation (conditional). Let $\mathcal{F}_n := \sigma(X_{1:n}, Y_{1:n})$. Since $\hat{\lambda}$ is \mathcal{F}_n -measurable and (X_{n+1}, Y_{n+1}) is independent of \mathcal{F}_n under both $P_{\text{train}}^n \otimes P_{\text{train}}$ and $P_{\text{train}}^n \otimes P_{\text{test}}$, the change-of-measure identity applies conditionally: for any \mathcal{F}_n -measurable random element $\tilde{\lambda}$,

$$\mathbb{E}_{P_{\text{test}}} \left[L(X, Y; \tilde{\lambda}) \mid \mathcal{F}_n \right] = \mathbb{E}_{P_{\text{train}}} \left[w(X, Y) L(X, Y; \tilde{\lambda}) \mid \mathcal{F}_n \right].$$

Applying this with $\tilde{\lambda} = \hat{\lambda}$ and $(X, Y) = (X_{n+1}, Y_{n+1})$ gives

$$\mathbb{E}_{P_{\text{test}}} \left[L(X_{n+1}, Y_{n+1}; \hat{\lambda}) \mid \mathcal{F}_n \right] = \mathbb{E}_{P_{\text{train}}} \left[L^w(X_{n+1}, Y_{n+1}; \hat{\lambda}) \mid \mathcal{F}_n \right].$$

Taking expectations over \mathcal{F}_n (i.e., over $(X_{1:n}, Y_{1:n}) \sim P_{\text{train}}^n$) yields

$$\mathbb{E}\left[L(X_{n+1}, Y_{n+1}; \hat{\lambda})\right] = \mathbb{E}\left[L^w(X_{n+1}, Y_{n+1}; \hat{\lambda})\right].$$

Combining with the bound from Step 2 completes the proof. \square

C Tighter Uniform Concentration Bounds via Variance-Sensitive Inequalities

The uniform concentration bound in Lemma 1 controls $\mathbb{E}[\sup_{\lambda \in \Lambda} |\hat{R}_n(\lambda) - R(\lambda)|]$ using Hoeffding’s inequality, yielding a leading term of order $B\sqrt{\log(2m)/(2n)}$. This bound depends only on the range B and ignores the variance of the losses entirely. When $\text{Var}(L_i(\lambda)) \ll B^2$ for most or all $\lambda \in \Lambda$ —a common situation in calibration and risk-control settings—variance-sensitive concentration inequalities can deliver substantially tighter bounds.

We present two refinements: a *Bernstein bound* that replaces the range B in the leading term with the worst-case standard deviation σ_{\max} (Appendix C.1), and an *empirical Bernstein bound* that replaces σ_{\max} with a data-driven estimate, requiring no knowledge of population quantities (Appendix C.2). We then propagate the improved bound through Theorem 1 (Appendix C.3) and provide a numerical comparison across variance regimes (Appendix C.4).

C.1 Bernstein-Type Uniform Concentration

Lemma 3 (Bernstein uniform concentration bound). *Let $\Lambda = \{\lambda_1, \dots, \lambda_m\}$ be a finite parameter set with $|\Lambda| = m < \infty$. For each $\lambda \in \Lambda$, let $L_1(\lambda), \dots, L_n(\lambda)$ be i.i.d. random variables satisfying*

$$0 \leq L_i(\lambda) \leq B \quad a.s.$$

Define

$$R(\lambda) = \mathbb{E}[L_1(\lambda)], \quad \hat{R}_n(\lambda) = \frac{1}{n} \sum_{i=1}^n L_i(\lambda), \quad \sigma^2(\lambda) = \text{Var}(L_1(\lambda)),$$

and set

$$\sigma_{\max}^2 = \max_{\lambda \in \Lambda} \sigma^2(\lambda).$$

Then

$$\mathbb{E}\left[\sup_{\lambda \in \Lambda} |\hat{R}_n(\lambda) - R(\lambda)|\right] \leq \sigma_{\max} \sqrt{\frac{2 \log(2m)}{n}} + \frac{B \log(2m)}{3n}.$$

Proof. For each $\lambda \in \Lambda$, define

$$Y_\lambda := \hat{R}_n(\lambda) - R(\lambda) = \frac{1}{n} \sum_{i=1}^n (L_i(\lambda) - \mathbb{E}[L_i(\lambda)]).$$

Then $\mathbb{E}[Y_\lambda] = 0$, and

$$Z := \sup_{\lambda \in \Lambda} |Y_\lambda| = \max\{Y_\lambda, -Y_\lambda : \lambda \in \Lambda\}.$$

Let $W_i(\lambda) := L_i(\lambda) - \mathbb{E}[L_i(\lambda)]$. Since $0 \leq L_i(\lambda) \leq B$ a.s., we have $|W_i(\lambda)| \leq B$ a.s. and $\text{Var}(W_i(\lambda)) = \sigma^2(\lambda)$. By Bernstein's mgf bound for bounded centered variables (see, e.g., [Boucheron et al., 2013, Theorem 2.10]), for all $\eta \in (0, 3n/B)$,

$$\log \mathbb{E}[e^{\eta Y_\lambda}] \leq \frac{\eta^2 \sigma^2(\lambda)/n}{2(1 - \eta B/(3n))}.$$

The same bound holds for $-Y_\lambda$. Hence every element in

$$\mathcal{Y} := \{Y_\lambda, -Y_\lambda : \lambda \in \Lambda\}$$

is sub-gamma with variance factor $v = \sigma_{\max}^2/n$ and scale parameter $c = B/(3n)$.

Applying a standard maximal inequality for sub-gamma variables (see, e.g., [Boucheron et al., 2013, Theorem 2.5]) to the collection \mathcal{Y} of size $2m$, we obtain

$$\mathbb{E}[Z] \leq \sqrt{2v \log(2m)} + c \log(2m).$$

Substituting $v = \sigma_{\max}^2/n$ and $c = B/(3n)$ gives

$$\mathbb{E} \left[\sup_{\lambda \in \Lambda} |\hat{R}_n(\lambda) - R(\lambda)| \right] \leq \sigma_{\max} \sqrt{\frac{2 \log(2m)}{n}} + \frac{B \log(2m)}{3n}.$$

□

Remark 2 (Variance ratio gain). *The ratio of the Bernstein leading term to the Hoeffding leading term is*

$$\frac{\sigma_{\max} \sqrt{2 \log(2m)/n}}{B \sqrt{\log(2m)/(2n)}} = \frac{2\sigma_{\max}}{B}.$$

When $\sigma_{\max} \ll B$ —for instance, if losses are concentrated near 0 or near a value well below B —this ratio can be much smaller than 1.

C.2 Empirical Bernstein Uniform Concentration

The Bernstein bound of Lemma 3 requires knowledge of σ_{\max}^2 . Following Maurer and Pontil [2009], the unknown variance $\sigma^2(\lambda)$ can be replaced by the empirical variance

$$\hat{\sigma}_n^2(\lambda) = \frac{1}{n} \sum_{i=1}^n (L_i(\lambda) - \hat{R}_n(\lambda))^2.$$

This yields a fully data-dependent concentration bound at the cost of slightly larger constants.

Lemma 4 (Empirical Bernstein Uniform Concentration). *Assume the same setup as in Lemma 3, define*

$$\hat{\sigma}_{\max} = \max_{\lambda \in \Lambda} \hat{\sigma}_n(\lambda).$$

Then for any $\delta \in (0, 1)$, with probability at least $1 - \delta$,

$$\sup_{\lambda \in \Lambda} |\hat{R}_n(\lambda) - R(\lambda)| \leq \hat{\sigma}_{\max} \sqrt{\frac{2 \log(2m/\delta)}{n}} + \frac{7B \log(2m/\delta)}{3(n-1)}.$$

This result follows from the empirical Bernstein inequality of Maurer and Pontil [2009] combined with a union bound over the collection $\{Y_\lambda, -Y_\lambda : \lambda \in \Lambda\}$. The factor $7/3$ in the second term (versus $1/3$ in Lemma 3) is the price paid for estimating the variance from data. Since $\hat{\sigma}_{\max}$ is computable from the calibration sample, this bound makes the adjusted selection threshold fully data-driven and adaptive to the observed loss variability.

Note that, unlike Lemma 3, this is a high-probability statement rather than an expectation bound, since the empirical variance $\hat{\sigma}_n^2(\lambda)$ is itself random.

C.3 Propagation to the Main Theorem

Substituting the Bernstein bound of Lemma 3 into the proof of Theorem 1 (specifically, replacing the Hoeffding-based Lemma 1 when bounding Term (I) of the three-term decomposition in Step 3) yields the following refinement.

Proposition 5. *Under the assumptions of Theorem 1, with*

$$\sigma_{\max}^2 = \max_{\lambda \in \Lambda} \text{Var}(L_i(\lambda)),$$

we have

$$\mathbb{E}[L_{n+1}(\hat{\lambda})] \leq \alpha + D_{\text{Bern}}(m, n),$$

where

$$D_{\text{Bern}}(m, n) = \sigma_{\max} \sqrt{\frac{2 \log(2m)}{n}} + \frac{B \log(2m)}{3n}.$$

The proof is identical to that of Theorem 1, with the single modification that Term (I) is bounded using Lemma 3 instead of Lemma 1. Terms (II) and (III) remain unchanged.

Applying the analogous adjusted selection rule with

$$\alpha'_{\text{Bern}} = \alpha - D_{\text{Bern}}(m, n)$$

yields

$$\mathbb{E}[L_{n+1}(\hat{\lambda}^{\text{adj}})] \leq \alpha.$$

Compared with the Hoeffding-based adjustment $\alpha' = \alpha - D(m, n)$, this Bernstein-based correction is less conservative whenever the loss variance satisfies $\sigma_{\max} < B/2$, reflecting the smaller intrinsic variability of the losses.

C.4 Numerical Comparison

We evaluate the three bounds in a regime representative of typical calibration settings: sample sizes $n \in \{1000, 2000, 5000, 10,000, 20,000\}$, $|\Lambda| = m = 200$ candidate hyperparameter values, and $B = 1$. Three variance regimes are considered: $\sigma_{\max}/B \in \{0.1, 0.3, 0.5\}$. For the empirical Bernstein bound, we set $\delta = 0.05$, use $\hat{\sigma}_{\max} = \sigma_{\max}$ (the oracle case), and evaluate the bound with $\log(2m/\delta)$ in place of $\log(2m)$. We also examine the sensitivity to m at fixed $n = 5000$.

Table 2: Excess risk bounds $D(m, n)$ for $B = 1$, $m = 200$. H = Hoeffding (Lemma 1), B = Bernstein (Lemma 3), EB = Empirical Bernstein (Lemma 4, $\delta = 0.05$).

n	$\sigma_{\max}/B = 0.1$			$\sigma_{\max}/B = 0.3$			$\sigma_{\max}/B = 0.5$		
	H	B	EB	H	B	EB	H	B	EB
1,000	.059	.013	.034	.059	.035	.061	.059	.057	.088
2,000	.042	.009	.020	.042	.024	.039	.042	.040	.058
5,000	.027	.005	.010	.027	.015	.022	.027	.025	.034
10,000	.019	.004	.006	.019	.011	.015	.019	.018	.023
20,000	.013	.003	.004	.013	.007	.010	.013	.012	.016

Table 3: Sensitivity to $|\Lambda| = m$ at fixed $n = 5,000$, $B = 1$, $\sigma_{\max}/B = 0.3$, $\delta = 0.05$.

m	Hoeffding	Bernstein	Emp. Bernstein
50	.024	.013	.020
100	.025	.014	.021
200	.027	.015	.022
500	.028	.016	.024

Discussion

Several observations emerge from the numerical comparison (Tables 2–3, Figures 5 and 6).

First, in this large- n , moderate- m regime, the Bernstein bound dominates the Hoeffding bound across all configurations. At $\sigma_{\max}/B = 0.1$ and $n = 5,000$, the Bernstein bound is roughly 5 times smaller (0.005 vs. 0.027), translating directly into a less conservative calibration threshold $\alpha' = \alpha - D(m, n)$ and a correspondingly less restrictive selection rule. Even at $\sigma_{\max}/B = 0.3$, the Bernstein bound is approximately 44% tighter than Hoeffding at $n = 5,000$.

Second, the empirical Bernstein bound is necessarily looser than the oracle Bernstein bound, owing to two factors: the additional $\log(1/\delta)$ term (since it is a high-probability bound evaluated at $\delta = 0.05$) and the larger constant $7/3$ in the second-order term. At small sample sizes, this gap can be substantial: at $n = 1,000$ with $\sigma_{\max}/B = 0.5$, the empirical Bernstein value (0.088) exceeds both the Hoeffding (0.059) and oracle Bernstein (0.057) bounds. However, the gap narrows rapidly with n , and by $n = 10,000$ the empirical Bernstein bound is competitive across all variance regimes.

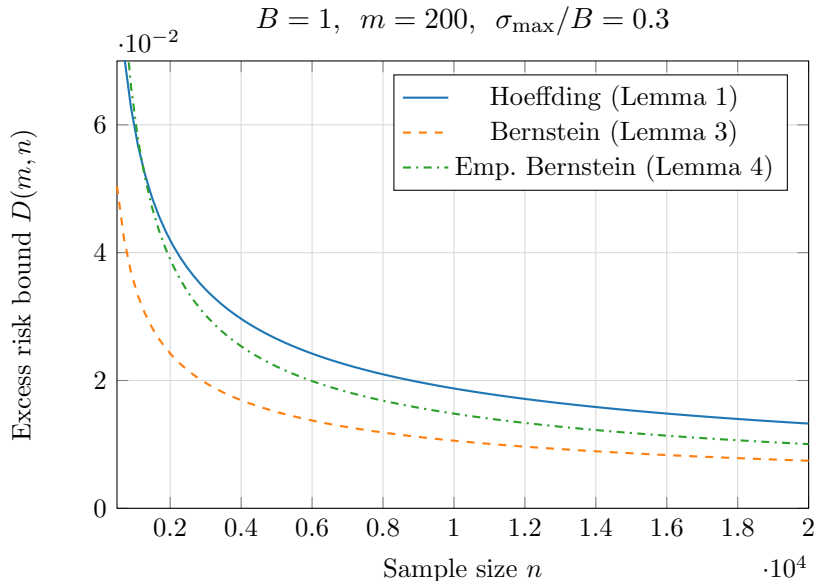


Figure 5: Excess risk bounds as a function of sample size for $\sigma_{\max}/B = 0.3$ and $m = 200$. The Bernstein bound (dashed) improves substantially over Hoeffding (solid) throughout the range $n \in [500, 20,000]$. The empirical Bernstein bound (dash-dotted, $\delta = 0.05$) tracks the oracle Bernstein bound at large n , with a larger gap at small n due to the variance estimation penalty and the additional $\log(1/\delta)$ factor.

In practice, one can take the pointwise minimum of the Hoeffding and empirical Bernstein bounds at no additional cost, ensuring the tighter bound is always used.

Third, Table 3 shows that the bounds are relatively insensitive to m over the range $m \in \{50, \dots, 500\}$ at $n = 5,000$, owing to the $\sqrt{\log m}$ dependence. Doubling m from 100 to 200 increases the Hoeffding bound by only 8% ($0.025 \rightarrow 0.027$) and the Bernstein bound by a comparable amount ($0.014 \rightarrow 0.015$). This is reassuring for applications where the hyperparameter grid is moderately large.

Fourth, all three bounds converge as $\sigma_{\max}/B \rightarrow 1$ (maximal variance), since the Bernstein inequality reduces to Hoeffding’s in the worst case. The practical implication is that the Bernstein refinement is most valuable precisely when calibration losses are well-behaved—a setting that is empirically common in conformal prediction and risk-controlling frameworks (see, e.g., Angelopoulos and Bates [2021], Bates et al. [2021]).

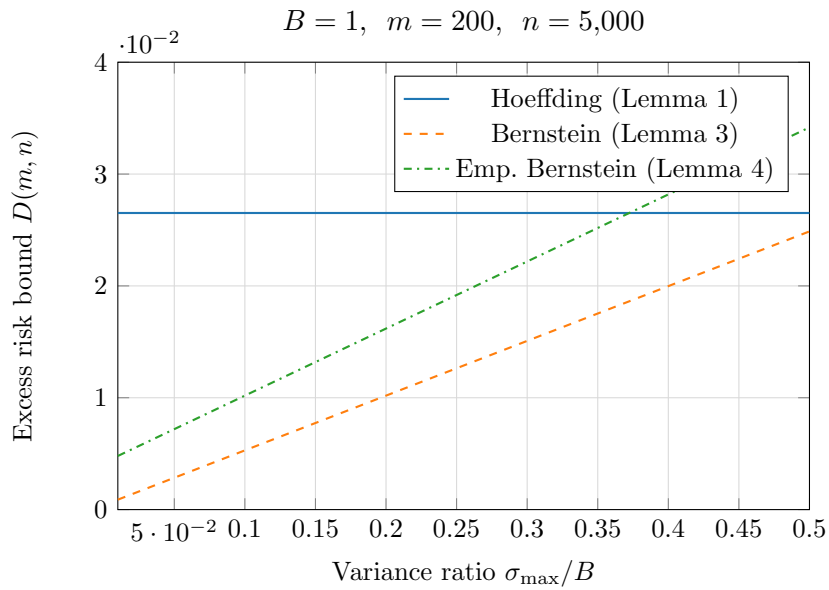


Figure 6: Excess risk bounds as a function of the variance ratio σ_{\max}/B at fixed $n = 5,000$ and $m = 200$. The Hoeffding bound (solid horizontal line) is variance-blind. Both Bernstein bounds decrease linearly in σ_{\max}/B , offering the largest gains in low-variance regimes. The empirical Bernstein bound ($\delta = 0.05$) has a steeper slope and larger intercept than the oracle Bernstein bound, reflecting the additional $\log(1/\delta)$ factor.

References

- Anastasios N Angelopoulos. Note on full conformal risk control. 2024.
- Anastasios N Angelopoulos. Conformal risk control for non-monotonic losses. *arXiv preprint arXiv:2602.20151*, 2026.
- Anastasios N Angelopoulos and Stephen Bates. A gentle introduction to conformal prediction and distribution-free uncertainty quantification. *arXiv preprint arXiv:2107.07511*, 2021.
- Anastasios N Angelopoulos, Amit Pal Kohli, Stephen Bates, Michael Jordan, Jitendra Malik, Thayer Alshaabi, Srigokul Upadhyayula, and Yaniv Romano. Image-to-image regression with distribution-free uncertainty quantification and applications in imaging. In *International Conference on Machine Learning*, pages 717–730. PMLR, 2022.
- Anastasios N Angelopoulos, Rina Foygel Barber, and Stephen Bates. Theoretical foundations of conformal prediction. *arXiv preprint arXiv:2411.11824*, 2024a.
- Anastasios N Angelopoulos, Stephen Bates, Adam Fisch, Lihua Lei, and Tal Schuster. Conformal risk control. In *The Twelfth International Conference on Learning Representations*, 2024b.
- Anastasios N Angelopoulos, Stephen Bates, Emmanuel J Candès, Michael I Jordan, and Lihua Lei. Learn then test: Calibrating predictive algorithms to achieve risk control. *The Annals of Applied Statistics*, 19(2):1641–1662, 2025. doi: 10.1214/24-AOAS1998.
- Rina Foygel Barber, Emmanuel J Candès, Aaditya Ramdas, and Ryan J Tibshirani. Conformal prediction beyond exchangeability. *The Annals of Statistics*, 51(2):816–845, 2023.
- Stephen Bates, Anastasios N Angelopoulos, Lihua Lei, Jitendra Malik, and Michael I Jordan. Distribution-free, risk-controlling prediction sets. *Journal of the ACM (JACM)*, 68(6):1–34, 2021.
- Stéphane Boucheron, Gábor Lugosi, and Pascal Massart. *Concentration Inequalities: A Nonasymptotic Theory of Independence*. Oxford University Press, Oxford, 2013.
- Kfir M Cohen, Sangwoo Park, Osvaldo Simeone, and Shlomo Shamai Shitz. Cross-validation conformal risk control. In *2024 IEEE International Symposium on Information Theory (ISIT)*, pages 250–255. IEEE, 2024.
- António Farinhas, Chrysoula Zerva, Dennis Ulmer, and André FT Martins. Non-exchangeable conformal risk control. *arXiv preprint arXiv:2310.01262*, 2023.
- Shai Feldman, Liran Ringel, Stephen Bates, and Yaniv Romano. Achieving risk control in online learning settings. *arXiv preprint arXiv:2205.09095*, 2022.

- Adam Fisch, Tal Schuster, Tommi Jaakkola, and Regina Barzilay. Conformal prediction sets with limited false positives. In *International Conference on Machine Learning*, pages 6514–6532. PMLR, 2022.
- Rina Foygel Barber, Emmanuel J Candes, Aaditya Ramdas, and Ryan J Tibshirani. The limits of distribution-free conditional predictive inference. *Information and Inference: A Journal of the IMA*, 10(2):455–482, 2021.
- Isaac Gibbs, John J Cherian, and Emmanuel J Candès. Conformal prediction with conditional guarantees. *Journal of the Royal Statistical Society Series B: Statistical Methodology*, page qkaf008, 2025.
- Jing Lei, Max G’Sell, Alessandro Rinaldo, Ryan J Tibshirani, and Larry Wasserman. Distribution-free predictive inference for regression. *Journal of the American Statistical Association*, 113(523):1094–1111, 2018.
- Andreas Maurer and Massimiliano Pontil. Empirical bernstein bounds and sample variance penalization. *Mathematics of Operations Research*, 34(2):287–314, 2009. doi: 10.1287/moor.1080.0339.
- Harris Papadopoulos, Kostas Proedrou, Vladimir Vovk, and Alexander Gammerman. Inductive confidence machines for regression. In *European Conference on Machine Learning*, pages 345–356. Springer, 2002.
- Aleksandr Podkopaev and Aaditya Ramdas. Distribution-free uncertainty quantification for classification under label shift. In *Uncertainty in artificial intelligence*, pages 844–853. PMLR, 2021.
- Tal Schuster, Adam Fisch, Tommi Jaakkola, and Regina Barzilay. Consistent accelerated inference via confident adaptive transformers. *arXiv preprint arXiv:2104.08803*, 2021.
- Glenn Shafer and Vladimir Vovk. A tutorial on conformal prediction. *Journal of Machine Learning Research*, 9:371–421, 2008.
- Jacopo Teneggi, Matthew Tivnan, Web Stayman, and Jeremias Sulam. How to trust your diffusion model: A convex optimization approach to conformal risk control. In *International Conference on Machine Learning*, pages 33940–33960. PMLR, 2023.
- Ryan J Tibshirani, Rina Foygel Barber, Emmanuel Candès, and Aaditya Ramdas. Conformal prediction under covariate shift. In *Advances in Neural Information Processing Systems*, volume 32, pages 2530–2540, 2019.
- Alexandre B. Tsybakov. *Introduction to Nonparametric Estimation*. Springer, 2009.
- Vladimir Vovk. Conditional validity of inductive conformal predictors. In *Asian conference on machine learning*, pages 475–490. PMLR, 2012.
- Vladimir Vovk, Alexander Gammerman, and Glenn Shafer. *Algorithmic Learning in a Random World*. Springer, 2005.

Volodya Vovk, Alexander Gammerman, and Craig Saunders. Machine-learning applications of algorithmic randomness. In *Proceedings of the Sixteenth International Conference on Machine Learning*, pages 444–453, 1999.